

---

This is an electronic reprint of the original article.  
This reprint may differ from the original in pagination and typographic detail.

Baniasadi, Hossein; Fathi, Ziba; Lizundia, Erlantz; Cruz, Cristina D.; Abidnejad, Roozbeh; Fazeli, Mahyar; Tammela, Päivi; Kontturi, Eero; Lipponen, Juha; Niskanen, Jukka

## Development and characterization of pomegranate peel extract-infused carboxymethyl cellulose composite films for functional, sustainable food packaging

*Published in:*  
Food Hydrocolloids

*DOI:*  
[10.1016/j.foodhyd.2024.110525](https://doi.org/10.1016/j.foodhyd.2024.110525)

Published: 01/01/2025

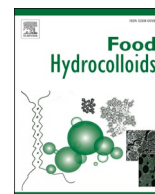
*Document Version*  
Publisher's PDF, also known as Version of record

*Published under the following license:*  
CC BY

*Please cite the original version:*  
Baniasadi, H., Fathi, Z., Lizundia, E., Cruz, C. D., Abidnejad, R., Fazeli, M., Tammela, P., Kontturi, E., Lipponen, J., & Niskanen, J. (2025). Development and characterization of pomegranate peel extract-infused carboxymethyl cellulose composite films for functional, sustainable food packaging. *Food Hydrocolloids*, 158, Article 110525. <https://doi.org/10.1016/j.foodhyd.2024.110525>

---

This material is protected by copyright and other intellectual property rights, and duplication or sale of all or part of any of the repository collections is not permitted, except that material may be duplicated by you for your research use or educational purposes in electronic or print form. You must obtain permission for any other use. Electronic or print copies may not be offered, whether for sale or otherwise to anyone who is not an authorised user.



# Development and characterization of pomegranate peel extract-infused carboxymethyl cellulose composite films for functional, sustainable food packaging

Hossein Baniasadi<sup>a,\*</sup>, Ziba Fathi<sup>b</sup>, Erlantz Lizundia<sup>c,d</sup>, Cristina D. Cruz<sup>e</sup>, Roozbeh Abidnejad<sup>b</sup>, Mahyar Fazeli<sup>b</sup>, Päivi Tammela<sup>e</sup>, Eero Kontturi<sup>b</sup>, Juha Lipponen<sup>b</sup>, Jukka Niskanen<sup>a</sup>

<sup>a</sup> Polymer Synthesis Technology, School of Chemical Engineering, Aalto University, Espoo, Finland

<sup>b</sup> Department of Bioproducts and Biosystems, School of Chemical Engineering, Aalto University, FI-00076, Aalto, Finland

<sup>c</sup> Life Cycle Thinking Group, Department of Graphic Design and Engineering Projects, Faculty of Engineering in Bilbao, University of the Basque Country (UPV/EHU), Bilbao, 48013, Spain

<sup>d</sup> BCMaterials, Basque Center for Materials, Applications and Nanostructures, UPV/EHU Science Park, 48940, Leioa, Spain

<sup>e</sup> Drug Research Program, Division of Pharmaceutical Biosciences, Faculty of Pharmacy, University of Helsinki, Viikinkaari 5E, 00790, Helsinki, Finland

## ARTICLE INFO

### Keywords:

Pomegranate peel extract  
Carboxymethyl cellulose  
Sustainable food packaging  
Life cycle assessment  
Antibacterial activity

## ABSTRACT

Our study explores the development and characterization of carboxymethyl cellulose (CMC)-based composite films integrated with clay particles and pomegranate peel extract (PE), aiming to inspire the films with natural antimicrobial and antioxidant properties for potential applications in food packaging. We conducted a comprehensive examination of the mechanical, barrier, surface, and degradation properties of these composite films, considering the impacts of incorporating clay particles and PE on their overall performance. Our findings reveal that the inclusion of clay particles enhances the mechanical strength and barrier properties of the films, while PE contributes to antioxidant and antibacterial effects. Namely, after the integration of 3 wt% clay, the tensile strength exhibited a remarkable increase of approximately 300%, accompanied by a notable reduction of 60% in water vapor permeability and 30% in oxygen transmission rate. Furthermore, the integration of PE into CMC films promoted antibacterial activity against 2 g-positive bacterial species, *Staphylococcus aureus* and *Listeria monocytogenes*. Additionally, we conducted a life cycle assessment (LCA) to quantify the cradle-to-gate environmental impacts of the developed bio-based active films. When normalized to the functional properties of the films, including mechanical and barrier performance, we observed significant benefits, with reductions of up to 59% after the concurrent incorporation of PE and clay nanosheets. Overall, our study underscores the potential of CMC-based composite films augmented with PE as a promising solution for sustainable food packaging, offering enhanced functionality while reducing environmental impact and increasing food safety.

## 1. Introduction

Food packaging is crucial for the food industry, serving essential roles for both consumers and producers. Its primary role lies in safeguarding food products from external contaminants and environmental factors, thus ensuring their safety, quality, and longevity. Traditional packaging films, such as polyethylene, have long been essential in the food industry due to their durability, flexibility, and barrier properties (Bahmanyar et al., 2015; Zia et al., 2019). However, their widespread use poses significant environmental challenges. They are mainly derived from petroleum, are non-biodegradable, and persist in the environment

for hundreds of years, contributing to pollution and ecosystem degradation. Moreover, a critical concern arises from microplastics, especially in aquatic ecosystems. Despite their convenience and effectiveness, the environmental impact of traditional packaging films like polyethylene underscores the urgent need for sustainable packaging solutions aimed at reducing waste and minimizing environmental impact throughout the packaging lifecycle (Asgher et al., 2020; Atta et al., 2022; Basbasan et al., 2022; Mohammadpour Velni et al., 2018).

Cellulose, a polysaccharide abundantly found in plant cell walls, has garnered significant attention for its potential in developing sustainable food packaging solutions. Derived from renewable sources such as

\* Corresponding author.

E-mail address: [hossein.baniasadi@aalto.fi](mailto:hossein.baniasadi@aalto.fi) (H. Baniasadi).

<https://doi.org/10.1016/j.foodhyd.2024.110525>

Received 14 June 2024; Received in revised form 24 July 2024; Accepted 12 August 2024

Available online 13 August 2024

0268-005X/© 2024 The Authors. Published by Elsevier Ltd. This is an open access article under the CC BY license (<http://creativecommons.org/licenses/by/4.0/>).

wood, cotton, or agricultural residues, cellulose offers inherent biodegradability and compostability, making it an environmentally friendly alternative to traditional petroleum-based plastics (Baniyadi et al., 2021; Fazeli, 2018; Zhu et al., 2024). Carboxymethyl cellulose (CMC), a derivative of cellulose, is particularly noteworthy for its versatility and functionality in various applications, including food packaging. CMC is obtained by the chemical modification of cellulose through carboxymethylation, which introduces carboxymethyl groups ( $-\text{CH}_2-\text{COOH}$ ) into the cellulose backbone. This modification enhances the solubility of cellulose in water and improves its film-forming properties. CMC-based films are known for their excellent mechanical strength and flexibility, which are crucial for maintaining the integrity of packaged food products (Behnezhad et al., 2020; Makam et al., 2024; Ramakrishnan et al., 2024; Yildirim-Yalcin et al., 2022).

While CMC offers numerous advantages as a potential material for food packaging, it also presents some drawbacks that need to be addressed. One significant drawback is its inherent brittleness (Viswanathan et al., 2024). CMC-based films can be prone to cracking or breaking under stress, particularly in dry conditions. Another drawback of CMC as a food packaging film is its relatively high water permeability rate (J. Yang, Li, et al., 2024). CMC films have a propensity to absorb moisture from the surrounding environment, leading to increased water permeation through the packaging film. This can pose challenges for preserving the quality and shelf life of moisture-sensitive food products, such as snacks, baked goods, or fresh produce, which may undergo undesirable changes in texture, flavor, or appearance when exposed to moisture. Additionally, high water permeability can result in issues such as package deformation, loss of product integrity, and increased susceptibility to microbial growth or spoilage (Kuchaiyaphum et al., 2024; Long et al., 2023). CMC can be functionalized or modified to enhance its performance, such as through chemical modifications or the incorporation of nanomaterials (C. Li, Zhang, et al., 2024; Shahbazi et al., 2016; K. Wang, Li, et al., 2024). However, to tackle the challenges presented by CMC-based food packaging films mentioned earlier, more environmentally friendly solutions can be employed. For instance, incorporating nanoparticles like clay to decrease water permeability and utilizing plasticizers like glycerin to enhance flexibility and reduce rigidity are potential approaches. By strategically combining these environmentally friendly approaches, CMC-based food packaging films can be tailored to meet specific requirements, offering a balance between moisture control, mechanical strength, and flexibility while still maintaining sustainability and biodegradability.

Moreover, utilizing plant extracts with inherent antimicrobial properties, such as pomegranate peel extract (PE), presents an innovative approach to developing active food packaging solutions (Latif et al., 2024; SG et al., 2023). PE contains bioactive compounds, including polyphenols and tannins, known for their antimicrobial properties against a wide range of foodborne pathogens and spoilage microorganisms (Kumar et al., 2022; Siddiqui et al., 2024). By incorporating PE into CMC-based packaging materials, such as films or coatings, it is possible to impart antimicrobial activity to the packaging, thereby extending the shelf life and ensuring the safety of packaged food products (Bodana et al., 2024; Cui et al., 2020). Additionally, active packaging systems incorporating plant extracts offer the advantage of being natural, sustainable, and environmentally friendly alternatives to synthetic antimicrobial agents (Makhathini et al., 2023). In line with this, various research groups have explored the integration of PE into CMC-based food packaging materials. For example, Ahmad et al. (Nabeel Ahmad et al., 2024) developed novel antioxidant and antibacterial composite films by blending PE with gelatin and CMC matrices. Their research demonstrated that these films effectively extended shelf life by up to 3 days, as indicated by reduced total viable counts, total volatile basic nitrogen, weight loss, and pH changes compared to control films. Similarly, Khalid et al. (Khalid et al., 2024) engineered free-standing CMC nanocomposite films infused with nanoencapsulated flavonoids from PE. Their findings showed that these nanocomposite

films exhibited superior antibacterial properties, prolonging the shelf life of beef and poultry meat by up to 12 days. Furthermore, researchers utilized pomegranate and citrus fruit peel extracts to synthesize green silver nanoparticles, which were then incorporated into cellulose-based packaging material as an environmentally friendly alternative to polyethylene-based packaging (Gopalakrishnan et al., 2023). Additionally, a multifunctional nanocomposite film consisting of CMC and pomegranate anthocyanin pigment was developed for food packaging purposes. This innovative film was found to extend the shelf life of red grapes and plums by up to 25 days while maintaining the fruits' quality better than unpackaged counterparts (El-Shall et al., 2023).

Many of the aforementioned research endeavors focused on developing and characterizing PE-containing films as a sustainable method for infusing natural antimicrobial and antioxidant properties into food packaging materials. The incorporation of environmentally sustainable materials into packaging films should be supported by standardized environmental impact assessment methodologies, which can substantiate claims of sustainability. In this regard, life cycle assessment (LCA), standardized by ISO 14040/44, offers a means to quantify the environmental impacts of materials (Berroci et al., 2022; Åkräs et al., 2024), processes (Iturondobeitia et al., 2022), or products (Peters et al., 2016) across various indicators such as greenhouse gas emissions, ecotoxicity, acidification, water use, and cumulative energy demand (Bovea & Pérez-Belis, 2012; Hellweg & Milà i Canals, 2014). Consequently, LCA is increasingly recognized as a valuable methodology for informing the environmentally sustainable design of materials, whether derived from non-renewable (Gironi & Piemonte, 2011; Peters et al., 2016) or renewable sources (Berroci et al., 2022; Z. Li et al., 2022).

In the current study, CMC was chosen as the base material, and its properties were enhanced by incorporating glycerol, clay nanosheets, and PE. The addition of clay nanosheets, which have been frequently used in developing food packaging films (Dharini et al., 2022; Nath et al., 2022), was specifically aimed at improving mechanical properties, reducing water vapor permeability (WVP), and enhancing the oxygen barrier properties of the films. Consequently, our findings demonstrated notable improvements in strength, stiffness, reduced WVP, and enhanced oxygen barrier properties following the integration of clay nanosheets. Moreover, we observed significant antioxidant and antibacterial effects against *Staphylococcus aureus*, particularly in films with higher PE content, making them potential candidates for extending the shelf life and ensuring the safety of perishable food products such as fresh produce, meat, or dairy items. More importantly, our study employed LCA to evaluate the sustainability profile of the developed bio-based active food packaging solution. Through LCA analysis, we confirmed the environmental benefits of our packaging system, further highlighting its potential to enhance food safety and prolong shelf life while reducing environmental impact across its life cycle.

## 2. Experimental

### 2.1. Materials

Carboxymethyl cellulose sodium salt (CMC, average molecular weight of 250,000 g/mol and degree of substitution of 0.7), glycerol (purity: >99.0%, GC), and 1-diphenyl-2-picrylhydrazyl free radical (DPPH) were purchased from Tokyo Chemical Industry Co. Clay (sodium montmorillonite, Na-MMT), citric acid monohydrate (CA), and sodium hypophosphite (SHP, 99%) were obtained from Sigma-Aldrich. Fresh pomegranate fruits were sourced from a local shop in Finland. Mueller Hinton Agar (MHA, Lab M Limited, Lancashire, UK) was procured from Neogen. Clinical bacterial strains *Escherichia coli* ATCC 25922 and *Staphylococcus aureus* ATCC 29213 were acquired from Microbiologics Inc. (St. Cloud, Minnesota, USA). *Listeria monocytogenes* DSM 112142 (isolated from minced meat) was sourced from the Leibniz Institute DSMZ German Collection of Microorganisms and Cell Culture. Cefaclor antimicrobial susceptibility discs (30 µg, Oxoid Ltd, Hampshire,

UK) were obtained from Thermo Fisher Scientific.

## 2.2. Pomegranate peel extraction

PE was prepared following the method outlined by Salim et al. (Salim et al., 2023). The peel of fresh pomegranate fruits was removed, and the arils were manually separated. The peel was then chopped into small pieces using a sharp knife and washed with distilled water. Subsequently, it was frozen at  $-30\text{ }^{\circ}\text{C}$  and dried under vacuum using a vacuum freeze dryer (Christ Alpha 2–4 Freeze Dryer) for 24 h at  $-55\text{ }^{\circ}\text{C}$ . The dried peel was ground into a fine powder using a coffee grinder. A portion of 1.5 g pomegranate powder was extracted with 30 mL ultra-pure water at  $40\text{ }^{\circ}\text{C}$  for 4 h in a thermostatic bath. The sample was centrifuged at 5000 rpm for 10 min, and the supernatant—comprising PE—was carefully collected and subsequently stored at  $5\text{ }^{\circ}\text{C}$  prior to use.

## 2.3. Composite film fabrication

For the preparation of pure CMC film, 1.5 g CMC was dissolved in 100 mL distilled water at ambient temperature under gentle mixing for 24 h. Subsequently, 0.375 g of glycerol, representing 25% of the dry mass of CMC (Afshar & Baniasadi, 2018), was added as a plasticizer, along with 0.15 g of CA, representing 10% of the dry mass of CMC, as a crosslinking agent to the solution. Additionally, a small amount of SHP was introduced as a catalyst to facilitate the direct crosslinking of CA with CMC (Dinesh et al., 2022). The mixing was continued for an additional hour. The solution was then left without stirring for 4 h to remove any formed bubbles. It was cast into a glass Petri dish and dried at ambient temperature for 24 h. The formed film was cured in an oven at  $70\text{ }^{\circ}\text{C}$  for 5 min.

To prepare clay-containing biocomposite films, a prescribed amount of clay was dispersed in 100 mL distilled water by 30 min of sonication, followed by another 30 min of mixing on a stirrer. The rest of the fabrication process was similar to that described for pure CMC film. The amount of clay in the biocomposite films was selected as 1%, 3%, and 5% of the mass of dry CMC, designated as CMC-C1, CMC-C3, and CMC-C5, respectively.

For the fabrication of PE-containing biocomposite films, one concentration of clay (CMC-C3) was selected, and 25 mL and 50 mL of the 100 mL distilled water used for the solution preparation were substituted with PE. The rest of the preparation conditions were similar to those for CMC film preparation. The PE-containing films were coded as CMC-C3-PE25 and CMC-C3-PE50, respectively.

## 2.4. Life cycle assessment

The environmental impacts associated with the manufacturing of bio-based active packaging were investigated using the life LCA methodology in accordance with ISO 14040/44 international standards (Laurent et al., 2020). The assessment encompassed the cradle-to-gate impacts, taking into account raw material acquisition, upstream processes, transport, energy consumption during processing, and waste management. Capital stock impacts resulting from equipment amortization were not included in the analysis. Energy consumption was estimated based on equipment power and usage time, assuming a 70% workload. Tables S1–S4 provide a summary of the life cycle inventory (LCI), presenting input and output data derived from laboratory experiments (primary data). Pomegranate peel was considered burden-free using the cut-off allocation method, although transportation over a distance of 100 km was accounted for, utilizing an EURO5 3.5–7.5 metric ton lorry from the source to the production site. Two energy use scenarios were considered: one utilizing the medium voltage current electricity mix of the European Network of Transmission System Operators (ENTSO-E), encompassing voltages between 1 kV and 24 kV, and accounting for infrastructure, losses, and transformation for the period 2015–2023; and the other utilizing medium voltage electricity from

fully renewable sources available in Switzerland in 2021, considering electricity inputs, transformation, transmission network, emissions, and losses. Table S5 presents the environmental impacts associated with the electricity mix. The assessment utilized the OpenLCA 2.1.1 software with the "ecoinvent v3.10 Cut-Off Unit Processes" database. The GaBi Bioplastics Database and the ReCiPe 2016Midpoint (H) methodology were used to evaluate the environmental impacts of bio-based composite materials with potential packaging applications. The details of the applied methodologies, as well as the functional units employed to standardize the impacts, are provided in the Supplementary Information (S1).

## 2.5. Film characterization

### 2.5.1. Fourier transform infrared spectroscopy

The functional groups present in the sample were analyzed using Fourier transform infrared (FTIR) spectroscopy conducted on a PerkinElmer FTIR instrument equipped with an Attenuated Total Reflectance (ATR) accessory. Scans were performed in transmittance mode over the wavenumber range of  $4000\text{ cm}^{-1}$ – $500\text{ cm}^{-1}$ , with a scan number of 16 and a resolution of  $4\text{ cm}^{-1}$ . Prior to measurement, the instrument was calibrated by recording the background signal under identical conditions.

### 2.5.2. Scanning electron microscope

The morphology of the sample was examined by imaging the cryo-fractured surface using a Zeiss Sigma VP scanning electron microscope (SEM). Before imaging, the sample surface was coated with a thin layer of gold-palladium (approximately 4 nm) and then imaged under a 3 kV voltage. Energy-dispersive spectroscopy (EDS) was employed alongside SEM to analyze the elemental composition of the sample. For this purpose, the acceleration voltage was increased to 20 kV. SEM was also utilized to observe surface morphology post-degradation testing.

### 2.5.3. Mechanical properties

The mechanical properties of the sample were evaluated using a Universal Tester Instron model 5944. Samples were punched into a dog-bone shape according to ASTM D882 type V tensile test specifications. Tensile testing was performed at a rate of 5 mm/min under ambient temperature using a 2 kN load cell. Typical stress-strain curves were generated, and key parameters such as tensile modulus (MPa), tensile strength (MPa), elongation at break (%), and toughness ( $\text{MJ}/\text{m}^3$ ) were derived and discussed. The toughness, representing the material's resistance to both fracture and deformation, was computed from the surface area under the stress-strain curves. Prior to testing, samples were conditioned at 55% relative humidity and  $23\text{ }^{\circ}\text{C}$  for 48 h. Each measurement was repeated five times, and the mean value with standard deviation was reported.

### 2.5.4. Water contact angle

The surface wettability of the sample was assessed by measuring the static contact angle of a water droplet using a Theta Flex Optical Tensiometer. A 5  $\mu\text{L}$  water droplet was deposited on the surface, and the contact angle was measured immediately after deposition and after 60 s. Reported contact angles to represent the average of at least three measurements.

### 2.5.5. UV-visible spectrometer

The film's transmittance property was assessed using a UV-3100 PC spectrophotometer (Shimadzu, Japan) at  $23\text{ }^{\circ}\text{C}$ . Scanning was conducted across the visible spectrum (400–700 nm). The transmittance at 600 nm was specifically considered (Zhang et al., 2024). Each film sample was cut into a 3 cm  $\times$  0.5 cm rectangular piece and directly attached to the wall of the cuvette for testing. Transparency (%) was calculated using Equation (1), where  $T_1$  represents the incident light intensity from the spectrophotometer source before interacting with the film sample

(100%), and  $T_2$  represents the transmitted light intensity through the film.

$$\text{Transparency (\%)} = \frac{T_2}{T_1} \times 100 \quad (1)$$

Each measurement was repeated at least three times, and the mean value with standard deviation was reported.

#### 2.5.6. Water vapor permeability

WVP was assessed according to ASTM D1653 using TQC Sheen Permeability Cups. Initially, a disk-shaped sample underwent drying in a vacuum oven at 60 °C for 24 h. Subsequently, it was weighed ( $m_0$ ) and placed into the permeability cup, pre-filled with a specific quantity of dried silica gel. The cup containing the sample was then positioned within a controlled humidity chamber set at 60% relative humidity and 24 °C. Over the course of 48 h, the weight changes of the cup ( $\Delta m = m_i - m_0$ ) were diligently monitored. A plot of  $\Delta m$  (g) against time (h) was generated, and a linear curve was interpolated from the data. From this curve, the slope was extracted ( $\Delta m/t$ , g/h), which was then utilized to calculate the WVP (g.m/m<sup>2</sup>/Pa/h) according to Equation (2) (Z. Li et al., 2023).

$$\text{WVP} = \frac{\text{Slope} \times d}{A \times \Delta P} \quad (2)$$

Where  $d$  represents film thickness (m),  $A$  is the area of the film through which water vapor transmits (0.001 m<sup>2</sup>), and  $\Delta P$  corresponds to saturated vapor pressure at 25 °C (3170 Pa).

#### 2.5.7. Oxygen transmission rate

In accordance with ASTM D 3985-95 standards, OTR experiments were performed at 23 °C and 50% relative humidity using a Mocon Oxtran 2/22 L Oxygen Permeability Analyzer (Mocon, Minneapolis, USA). The samples, with an approximate area of 5.5 cm<sup>2</sup>, were subjected to an oxygen partial pressure of 1 atm. To derive the oxygen permeation, the OTR was standardized by considering the sample area, oxygen pressure, and material thickness.

#### 2.5.8. Degradation study

The degradation of the sample was investigated through a soil burial experiment using Garden black soil Biolan. Initially, the sample underwent drying in a vacuum oven at 60 °C for 24 h to remove any moisture. Subsequently, it was weighed ( $m_0$ ) and buried in the soil. The experiment was conducted in late winter, specifically in January 2024, as depicted in Fig. S1, illustrating the experimental setup. Throughout the conditioning period, the soil beds were regularly watered as required and mixed to ensure consistent moisture distribution. Weekly intervals saw the removal of the sample, followed by cleaning its surface using blotter paper and reweighing ( $m_i$ ). The degradation rate ( $D$ ) was then calculated using Equation (3).

$$D(\%) = \frac{m_0 - m_i}{m_0} \times 100 \quad (3)$$

#### 2.5.9. Antioxidant activity

The antioxidant activity (AOA) of the produced mats was assessed through a 1,1-diphenyl-2-picrylhydrazide (DPPH) assay. Initially, a 10 µg/mL DPPH ethanolic solution was prepared, with an initial absorbance ( $A_0$ ) measured at a wavelength of 517 nm. Subsequently, the film was immersed in 3.0 mL of the prepared DPPH solution. The system was then incubated in darkness at room temperature for various durations, including 30 min, 1 h, 2 h, 3 h, and 24 h. Following incubation, the absorbance of the DPPH solution ( $A_s$ ) was re-measured at 517 nm. The AOA of the film was determined using the following equation.

$$\text{AOA(\%)} = \frac{A_0 - A_s}{A_0} \times 100 \quad (4)$$

#### 2.5.10. Antibacterial assay

All bacterial strains were stored at −80 °C, with working cultures maintained on MHA plates at 2–8 °C. The antibacterial properties of the films were assessed using the Kirby-Bauer disk diffusion method (CLSI M02-A12 and CLSI M100-S26, n.d.). Briefly, pre-cut discs of films (approximately 7 mm in diameter) were sterilized under UV light for 15 min. Fresh bacteria were cultured on MHA plates at 37 °C for 16–20 h before the assay. A few colonies from the overnight culture on MHA plates were inoculated into 0.9% saline solution and vortexed to ensure homogeneity of the bacterial suspension. The bacterial suspensions were standardized to a 0.5 McFarland standard using a DEN-1 densitometer (BioSan), equivalent to a bacterial suspension containing approximately 1–2 × 10<sup>8</sup> colony-forming units (CFU/mL). A sterile cotton swab was dipped into the bacterial suspension and used to inoculate three replicate MHA plates per bacterial strain, ensuring even distribution. Films were then applied to the surface using a sterile forcep and gently pressed against the agar. The MHA plates were incubated for 24 h at 37 °C. Cefaclor (30 µg) served as the positive control, while CMC and CMC-C3 films served as negative controls on every assay plate. The diameter of the zones of growth inhibition was measured using a caliper (in mm), with the size of the discs subtracted from the final measurements and average values reported. Initial screening experiments were performed once in triplicate. For films exhibiting antibacterial activity (i.e., formation of a zone of inhibition), experiments were repeated two more times in triplicate. Statistical analysis was conducted using OriginPro Graphing and Analysis software, version 2021b (OriginPro). Mean values of the zone of inhibition were analyzed using ANOVA followed by pairwise post-hoc Tukey test to analyze differences between films within the same bacterial group. Significant differences were considered when  $p < 0.05$ .

### 3. Results and discussion

#### 3.1. Chemical structure study

FTIR spectra were employed to identify the primary signals of the functional groups present in the precursors and the films. The spectra are depicted in Fig. 1. Prior to curing, the spectrum of CMC exhibited absorption peaks in the wavenumber region of 3500–3000 cm<sup>−1</sup>, attributed to stretching vibrations in hydroxyl groups. Additionally, two discernible peaks were observed at 2901 cm<sup>−1</sup> and 2893 cm<sup>−1</sup>, corresponding to aliphatic C–H bond stretching in alkyl groups. Moreover, the peak at 1584 cm<sup>−1</sup> indicated the symmetric and asymmetric carboxyl groups of CMC, while peaks at 1419 cm<sup>−1</sup>, 1315 cm<sup>−1</sup>, and 1012 cm<sup>−1</sup> signified the presence of –OH, C–H, and C–O bonds, respectively. Collectively, these characteristics delineate the structure of the CMC polysaccharide (Fernández-Santos et al., 2022). In the cured CMC film, a band at 1720 cm<sup>−1</sup> emerged, aligning with the stretching vibration of carboxyl and ester carbonyl C=O, thereby confirming the esterification reaction of CA and CMC (de Cuadro et al., 2015; Liu et al., 2024). According to the literature (Vargas-Torrico et al., 2022), the glycerol spectrum reveals a broad peak at 3271 cm<sup>−1</sup> associated with the stretching vibration of the –OH groups, along with peaks at 2940 cm<sup>−1</sup> and 2884 cm<sup>−1</sup> corresponding to the C–H bond of the methyl group and peaks at 1648 cm<sup>−1</sup>, 1415 cm<sup>−1</sup>, and 1034 cm<sup>−1</sup>, attributed to the hydroxyl groups as well as C–OH and C–O–C bonds. Although most of these peaks overlapped with those of CMC, the presence of a distinct peak at 3271 cm<sup>−1</sup> in the spectrum of the cured CMC film suggests the presence of glycerol in the film.

The clay particles exhibited characteristic bands consistent with those documented in the literature (Elmahdy & Yassin, 2024). Specifically, a distinct transmission band appeared at 3620 cm<sup>−1</sup>, attributed to the stretching vibration of the –OH group. Another notable feature was the peak observed at 1635 cm<sup>−1</sup>, originating from bending OH vibrations. Moreover, the stretching vibrations of SiO were evident at

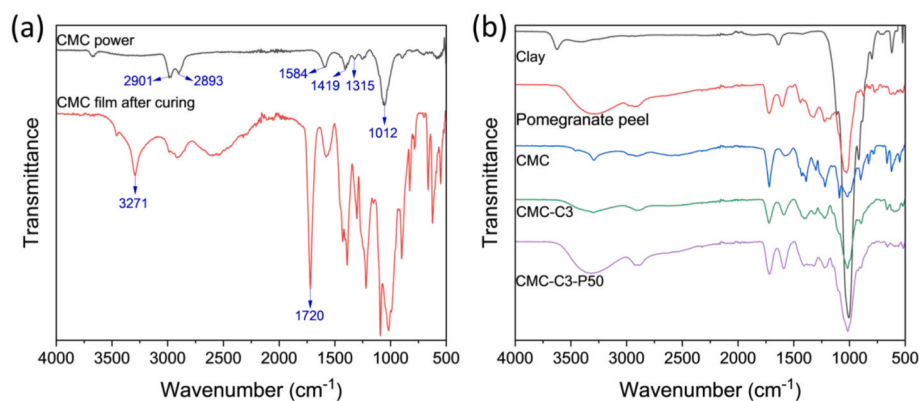


Fig. 1. FTIR spectra comparing CMC powder, clay, pomegranate peel powder, and CMC along with select composite films.

wavenumbers of  $1035\text{ cm}^{-1}$  and  $990\text{ cm}^{-1}$ . Additionally, three bands located at  $920\text{ cm}^{-1}$ ,  $875\text{ cm}^{-1}$ , and  $850\text{ cm}^{-1}$  were attributed to the OH bending modes. Likewise, according to the literature (Bertolo et al., 2022), the significant characteristic peaks of pomegranate peel powder include broadband associated with the stretching of the  $\text{-OH}$  bonds of alcohol, phenol, and carboxylic groups present in phenolic compounds at  $3290\text{ cm}^{-1}$ , a slight band at  $2915\text{ cm}^{-1}$  corresponds to the C-H stretching of methyl, methoxyl, and methylene groups found in phenolic acids, two neighboring bands at  $1722\text{ cm}^{-1}$  and  $1604\text{ cm}^{-1}$  represent the C=O bonds present in carbonyls and the C=C bonds of aromatic rings, respectively, and three bands at  $1340\text{ cm}^{-1}$ ,  $1205\text{ cm}^{-1}$ , and  $1030\text{ cm}^{-1}$  attribute to the stretching of N-H bonds in secondary amines, C-H in aromatics, and C-C-N in amines. Although some of the mentioned peaks overlapped with those previously reported for CMC, several could be distinctly detected in the FTIR spectra of composite films. For example, the peaks observed at  $1035\text{ cm}^{-1}$  and  $1604\text{ cm}^{-1}$  indicated the presence of clay and pomegranate peel, respectively.

### 3.2. Transparency study

Transparency in food packaging films is essential for consumer appeal, trust, and effective product marketing. Transparent packaging allows consumers to view the product inside, enabling them to assess its quality, freshness, and quantity, which increases the likelihood of purchase (Zhang et al., 2024). Fig. 2a presents the UV-Vis spectra of the fabricated film from 400 nm to 700 nm, while Fig. 2b

depicts the transparency of the films measured at 600 nm. The CMC film demonstrated high optical transparency, exceeding 70% within the wavelength range of 400 nm–700 nm. Specifically, at 600 nm, it exhibited a transparency of  $80.28 \pm 3.01\%$ , consistent with literature values for CMC films used in food packaging (Fernández-Santos et al., 2022). This level of transparency ensures a clear view of the packaged items (W. Li, Zhang, et al., 2024).

The introduction of clay particles reduced transparency, likely due to increased light scattering and absorption from the clay in the film matrix (El Mouzahim et al., 2023). The film with the highest clay loading, CMC-C5, showed a transparency of  $59.26 \pm 2.02\%$ . However, after incorporating PE, transparency improved compared to the control film, CMC-C3. Specifically, transparency was  $73.72 \pm 2.75\%$  in CMC-C3-P25 and  $64.46 \pm 2.11\%$  in CMC-C3-P50, compared to  $64.98 \pm 2.65\%$  in CMC-C3. Soleimanzadeh et al. (Soleimanzadeh et al., 2024) reviewed the effects of PE on the transparency of polymer matrices in active packaging films containing pomegranate peel and noted mixed results. Some studies reported reduced transparency with PE addition, while others observed an increase, and some found no significant effect. In our study, the observed increase in transparency with PE incorporation may be attributed to the formation of a more uniform film structure that reduces light scattering. Additionally, the bioactive compounds in PE, such as polyphenols and tannins, might interact with the CMC matrix, potentially leading to a more organized molecular structure that enhances light transmission. Further investigation is needed to fully understand the mechanisms behind the increased film transparency with

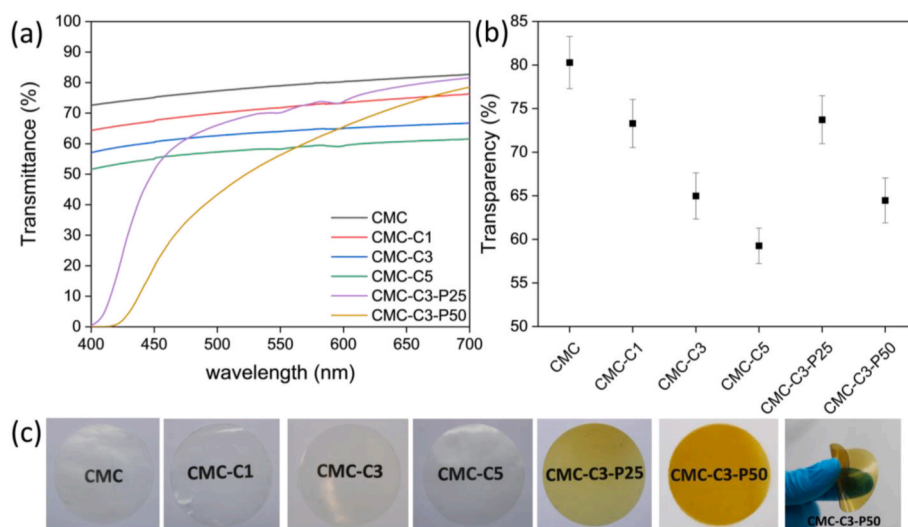


Fig. 2. (a) Digital images showcasing the fabricated films. (b) UV-Vis spectra (the scanning was performed at  $23\text{ }^{\circ}\text{C}$  from 400 to 700 nm). (c) Transparency of the films at  $23\text{ }^{\circ}\text{C}$  and a wavelength of 600 nm.

PE. It is also noteworthy that, as shown in the digital photos of CMC-based films (Fig. 2c), the color shifted from colorless to yellowish-brown with PE addition. Despite this color change, the films retained good transparency, allowing clear visibility of the product names.

UV light can negatively affect food quality by degrading nutrients and antioxidants and oxidizing lipids. Prolonged exposure to UV rays and excessive sunlight can significantly reduce food quality and shelf life. Therefore, the ability to block UV radiation is crucial for food packaging materials (Rochima et al., 2024). In the PE-containing films, the transmittance dropped to nearly zero around 400 nm, indicating their potential to block UV light and suggesting their effectiveness in

preventing photochemical reactions in food (Fernández-Santos et al., 2022).

### 3.3. Microstructure study

SEM images were employed to investigate the microstructure and surface morphology of the composite films. The SEM images from the cryofracture surface area of the films, as well as the elemental mapping images, are illustrated in Fig. 3. The SEM analysis of the pure CMC film revealed a smooth and homogeneous surface morphology. The surface appeared devoid of significant irregularities or roughness, indicating a uniform composition and structure throughout the film. The absence of

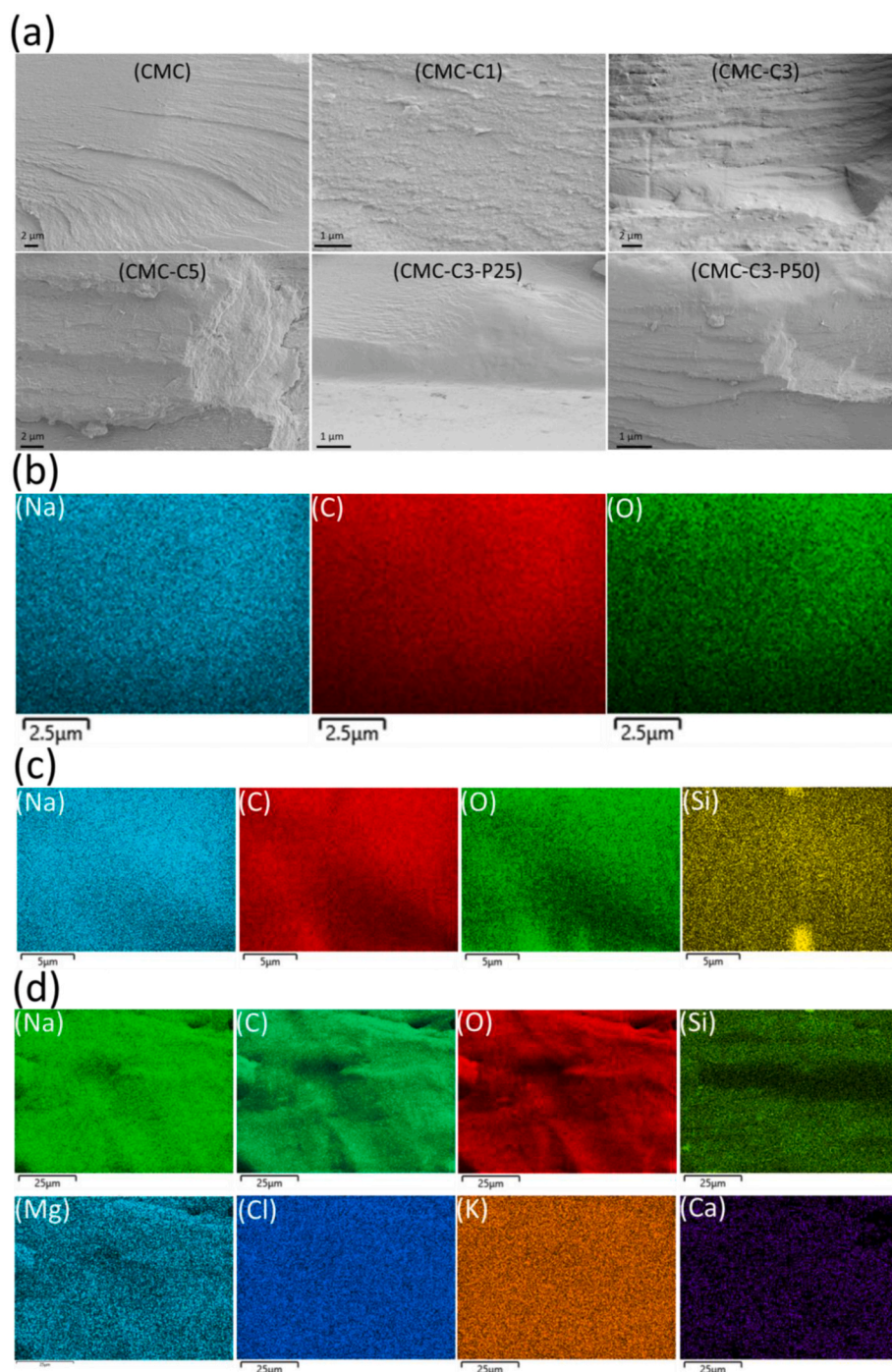


**Fig. 3.** (a) SEM images captured from the cryofracture surface area of the fabricated films. The elemental mapping images of (b) CMC, (c) CMC-C3, and (d) CMC-C3-P50 films.

visible particles or clusters suggested a lack of filler materials or additives within the cellulose matrix. However, the SEM analysis of the fracture surface area of the composite films revealed a heterogeneous surface with irregularities and roughness, indicative of the presence of filler particles within the CMC matrix. Clusters of particles, likely representing the dispersed clay reinforcement, were observed throughout the surface, suggesting a uniform distribution within the film matrix. As depicted in Fig. S2, the employed clay particle size ranged from a few microns to a few hundred microns. Nonetheless, under the employed magnification, i.e., 10kx, no sign of particle agglomeration could be detected in the composite films. The absence of particle agglomeration suggests that the clay particles were well dispersed and effectively incorporated into the cellulose matrix during the film preparation process, contributing to enhanced mechanical properties and structural integrity of the composite film. Additionally, no sign of cracks, voids, or phase separation could be detected, further proving the effective integration of the clay nanoparticles with the cellulose matrix. It should be highlighted that in the SEM images provided from PE-containing composite films, no clear differences could be seen, indicating the presence of PE did not significantly alter the surface morphology or structure of the composite films.

EDS was used for elemental map-scanning analysis to measure elemental percentages and obtain elemental mapping images for CMC, CMC-3, and CMC-3-P50 films. The elemental percentages are tabulated in Table S6, while the elemental mapping images are depicted in Fig. 3. The mapping images visually indicated a smooth surface morphology with several main components. Specifically, in the CMC film, the major elements measured by EDS were Na (14.08%), C (67.05%), and O (18.88%). In the clay-containing films, the presence of Si was also detected, confirming the existence of elemental silicon from the incorporated clay particles. Furthermore, the mapping images visually validated that silicon was uniformly distributed in the scanning area, reflecting the uniform distribution of clay particles.

### 3.4. Mechanical properties

The mechanical properties of films intended for food packaging are pivotal in ensuring product integrity, extending shelf life, and safeguarding against physical damage during handling, transportation, and

storage. Consequently, the tensile mechanical properties of these films were meticulously measured and analyzed. Fig. 4a and b depict the typical stress-strain curves, while Table 1 summarizes the relevant data extracted from these curves. The mechanical properties of the pure CMC film, including tensile modulus, tensile strength, and elongation at break, were found to be consistent with those reported for CMC films plasticized with glycerol (Lv et al., 2024; Vargas-Torrico et al., 2024). Upon the incorporation of clay particles, the tensile modulus and tensile strength showed a systematic increase, while the elongation at break decreased. For instance, the tensile modulus and tensile strength increased from  $134 \pm 5$  MPa and  $12.9 \pm 0.4$  MPa in the CMC film to  $1055 \pm 40$  MPa and  $37.5 \pm 1.0$  MPa in the CMC-C3 composite film, respectively. However, the elongation at break reduced from  $23.5 \pm 1.0\%$  to  $18.0 \pm 0.8\%$ . In essence, the presence of clay particles led to significant enhancements in mechanical strength and stiffness while reducing the film's flexibility and extensibility. These improvements in mechanical properties validate that the uniformly distributed clay particles acted as reinforcing agents within the CMC matrix, effectively distributing stress and preventing crack propagation, thereby enhancing tensile strength and modulus (Majumder et al., 2023). Moreover, the high aspect ratio and large surface area of the clay particles facilitated strong interfacial interactions with the polymer matrix, resulting in improved load transfer and adhesion, further enhancing mechanical properties (Zeng et al., 2024). Additionally, the establishment of hydrogen bonding between the clay particles and the cellulose matrix

**Table 1**  
Mechanical properties of the films extracted from stress-strain curves.

Sample	Tensile modulus (MPa)	Tensile strength (MPa)	Elongation at break (%)	Toughness (MJ/m <sup>3</sup> )
CMC	$134 \pm 5$	$12.9 \pm 0.4$	$23.5 \pm 1.0$	$174 \pm 7$
CMC-C1	$525 \pm 22$	$19.5 \pm 0.6$	$11.6 \pm 0.4$	$157 \pm 6$
CMC-C3	$1055 \pm 40$	$41.0 \pm 1.3$	$18.0 \pm 0.8$	$483 \pm 20$
CMC-C5	$1359 \pm 51$	$37.5 \pm 1.0$	$15.3 \pm 0.5$	$394 \pm 15$
CMC-C3-P25	$870 \pm 32$	$35.8 \pm 1.0$	$11.4 \pm 0.4$	$267 \pm 10$
CMC-C3-P50	$1110 \pm 40$	$33.7 \pm 1.0$	$7.8 \pm 0.3$	$183 \pm 7$

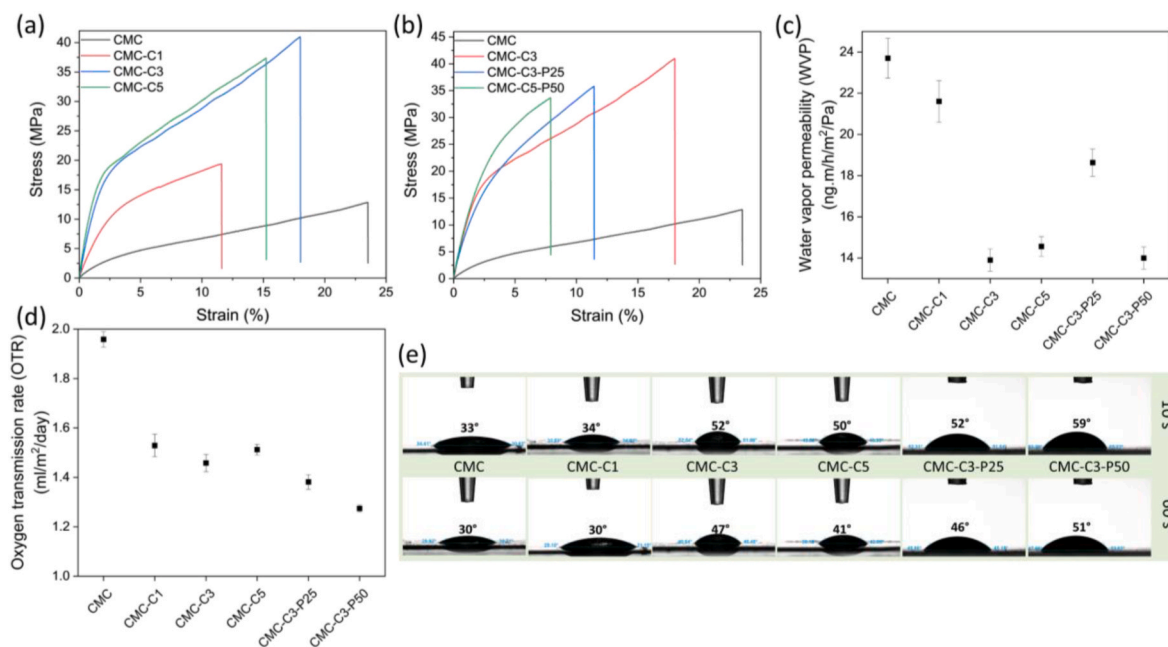


**Fig. 4.** (a) and (b) Typical stress-strain curves. (c) Water vapor permeability (WVP) and (d) oxygen transmission rate (OTR) results. (e) The water contact angle results from 10 to 60 s after water droplet deposition.

contributed to the enhanced mechanical performance (El Mouzahim et al., 2023).

The elongation at break decreased upon the introduction of clay particles, indicating that the presence of clay particles restricted polymer chain mobility, thereby reducing chain slippage and increasing resistance to deformation. Furthermore, the toughness improved significantly upon the addition of clay particles, implying that the composite film became more resistant to deformation and exhibited greater energy absorption capacity before failure. This enhancement in toughness suggests that the clay particles effectively reinforced the polymer matrix, mitigating crack propagation and enhancing the film's ability to withstand mechanical stress without catastrophic failure. It should be noted that the mechanical properties began to decline at a higher clay concentration of 5 wt% potentially due to particle agglomeration within the polymer matrix. Although SEM images did not reveal any particle agglomeration (Fig. 3a), the likelihood of particle agglomeration increased with higher clay concentrations, leading to localized areas of stress concentration and decreased mechanical performance. This aggregation of clay particles can disrupt the uniform dispersion and distribution within the polymer matrix, resulting in compromised load transfer and structural integrity, consequently diminishing the film's ability to resist deformation and withstand mechanical stress. Upon the incorporation of PE, the mechanical properties were reduced, rendering the film more brittle. PE likely interacted with the polymer chains, disrupting cohesive forces and hindering load transfer between them. This interaction may have decreased polymer chain mobility, resulting in a more rigid and less flexible film. Nonetheless, the observed mechanical properties of the PE-containing composite films were consistent with those reported for bio-based films used in food packaging applications (Riahi et al., 2024; Tanwar et al., 2021).

It is essential to highlight that the observed mechanical properties of the composite films align with those reported for bio-based packaging films. For instance, Abdin et al. (Abdin et al., 2024) reported tensile strengths ranging from 15 MPa to 70 MPa and elongation at break ranging from 1.5% to 4% for 235-ferulic acid-loaded polyethylene glycol/carboxymethyl cellulose films. Similarly, Khan et al. (Khan et al., 2024) observed a tensile strength as high as 1 MPa and elongation at break of 30% in packaging films composed of chitosan and natural berry wax. Additionally, a tensile strength of  $23.80 \pm 0.29$  MPa and tensile strain of  $18.61 \pm 0.34\%$  were reported for edible film packaging made from corn starch, sodium alginate, and  $\kappa$ -carrageenan (Y.-C. Yang, Li, et al., 2024). Furthermore, the tensile strength and tensile modulus of modified cellulose nanocrystals/polycaprolactone films were reported to be in the range of 25–32 MPa and 120–470 MPa, respectively (Alkassfarity et al., 2024). Recent research reported the tensile strength and tensile modulus of CMC-based films developed for food packaging as 45.4 MPa and 917 kPa, respectively (Hou et al., 2024). Additionally, the maximum tensile stress of 36.80 MPa and strain of 19.42% were achieved for CMC film crosslinked with 1% polyethylenimine (C. Li, Zhang, et al., 2024). Mukherjee et al. (Mukherjee et al., 2024) also reported a tensile strength and tensile modulus as high as  $9.86 \pm 0.14$  MPa and  $89.02 \pm 1.59$  MPa for CMC edible films containing cetylcaprylate.

### 3.5. Water vapor permeability and oxygen transmission rate

WVP and OTR play a crucial role in both the design and functionality of food packaging films, serving as vital parameters in preserving the quality and prolonging the shelf life of packaged food products. Therefore, the WVP and OTR of the developed films were examined. The WVP values are depicted in Fig. 4c, with detailed calculations provided in Fig. S3. Similarly, the OTR results are plotted in Fig. 4d. Notably, the CMC film exhibited the highest WVP, measured at  $23.7 \pm 0.97$  ng m/h/m<sup>2</sup>/Pa. This observation may be attributed to the presence of free hydroxyl groups within the film, which exhibit an affinity toward atmospheric moisture, thereby facilitating its transmission through the film (Chakraborty et al., 2023). Likewise, the highest OTR value was

observed in the CMC film, measuring  $1.96 \pm 0.03$  mL/m<sup>2</sup>/day. A systematic reduction in both WVP and OTR was observed upon the introduction of clay particles. Specifically, CMC-C3 composite films demonstrated a relatively low WVP and OTR of  $14.56 \pm 0.47$  ng m/h/m<sup>2</sup>/Pa and  $1.46 \pm 0.03$  mL/m<sup>2</sup>/day, respectively. This reduction can be attributed to the enhanced barrier properties conferred by the incorporation of clay particles into the film matrix. The intercalation of clay within the polymer matrix creates tortuous pathways for water vapor and oxygen molecules, impeding their diffusion through the material (Riahi et al., 2024; Velásquez et al., 2024; Zeng et al., 2024). Additionally, the presence of clay particles may contribute to forming a denser film structure with decreased free volume of the polymeric matrix, further limiting the permeation of water vapor and oxygen (El Bourakadi et al., 2022; Long et al., 2023). Furthermore, as proposed by Upadhyay et al. (Upadhyay et al., 2022), this reduction could possibly be due to the reduced availability of the free hydroxyl group of CMC for water molecules as a result of the involvement of CMC hydroxyl groups in hydrogen bonding with surface silanol (SiOH) groups of clay. Consequently, the observed decrease in WVP signifies an improvement in the moisture barrier performance of the composite films, enhancing their efficacy in preserving the quality and freshness of packaged food products over extended storage periods.

The WVP rate exhibited a slight increase in the composite film containing 5 wt% clay, which could be attributed to clay agglomeration within the polymer matrix, as previously observed in the mechanical properties results and also reported by other research groups (Mao et al., 2022). At higher clay concentrations, there is a greater likelihood of particle clustering or agglomeration, leading to localized areas of increased pathways for moisture to penetrate the film. In the PE-containing composite films, WVP increased in CMC-C3-P25; however, it decreased again in CMC-C3-P50. Our observation aligns with Tanwar et al. (Tanwar et al., 2021), who reported an increase in the WVP of polyvinyl alcohol/corn starch film upon the introduction of coconut shell extract. At lower concentrations of PE (CMC-C3-P25), the incorporation of PE may have disrupted the polymer matrix, creating additional pathways for water vapor transmission. However, as the concentration of PE increased (CMC-C3-P50), it likely formed a more cohesive and continuous phase within the film, thereby enhancing the barrier properties and reducing WVP. Nevertheless, further investigation is warranted to thoroughly comprehend the mechanism underlying the change in WVP upon the introduction of PE. On the other hand, OTR was slightly reduced upon the incorporation of PE. PE contains bioactive compounds such as polyphenols, flavonoids, and tannins, which possess antioxidant properties. These antioxidants have the capability to scavenge free radicals, including oxygen radicals, thereby reducing the rate of oxidative reactions that lead to the degradation of the packaging material (Nabeel Ahmad et al., 2024; Soleimanzadeh et al., 2024). Furthermore, the addition of PE may contribute to the formation of a protective barrier within the packaging film. This barrier could hinder the diffusion of oxygen molecules through the film, effectively reducing the OTR.

The water vapor transmission rate (WVT) of the developed films was calculated based on WVP values, ranging from 5.6 g/m<sup>2</sup>/day to 21.4 g/m<sup>2</sup>/day. Meanwhile, the OTR ranged from 1.26 mL/m<sup>2</sup>/day to 1.96 mL/m<sup>2</sup>/day. It is important to highlight that both OTR and WVT values for the developed composite films are highly promising. These values nearly meet the optimal target values for more vulnerable food products, which are around 10 g/m<sup>2</sup>/day for WVT and 10 mL/m<sup>2</sup>/day for OTR, constituting the critical zone for perishable food preservation (Godoy Zúniga et al., 2024).

### 3.6. Surface wettability study

The study of surface wettability plays a crucial role in the design and development of food packaging materials. Specifically, the surface wettability of packaging materials affects their ability to repel or absorb

liquids, thereby influencing their barrier properties. Moreover, surface wettability impacts the potential for microbial growth and contamination on the packaging surface. Accordingly, the surface wettability of the developed films was investigated by measuring the contact angle of deposited water at both 10 s and 60 s after positioning. The digital images are depicted in Fig. 4e. The CMC exhibited an average water contact angle of 33° and 30° after 10 s and 60 s of deposition, respectively. This low water contact angle indicates a hydrophilic surface attributed to the abundance of hydroxyl groups in the CMC polymer chain. These hydroxyl groups readily interact with water molecules, resulting in the observed low contact angle (Lee et al., 2024). The introduction of clay particles led to an increase in the water contact angle, rising to 52 °C in CMC-C3 composite films. Clay particles can improve the barrier properties of the film by creating a more tortuous path for water molecules, thus reducing water absorption. This reduced absorption can manifest as an increased contact angle (Jali et al., 2023).

Furthermore, upon the incorporation of PE, the water contact angle increased to 60°, which can be attributed to the presence of bioactive compounds such as polyphenols, flavonoids, and tannins in the extract. These compounds possess hydrophobic properties, which contribute to the increase in water contact angle by modifying the surface chemistry of the film (Bertolo et al., 2022; Nabeel Ahmad et al., 2024). Conversely, polyphenols and tannins are rich in hydroxyl groups and can form hydrogen bonds with cellulose, potentially decreasing the hydrophilicity of the film surface exposed to water. Additionally, the formation of a protective barrier by PE within the packaging material may alter the surface properties, resulting in reduced interaction with water molecules and, consequently, a higher water contact angle.

There are a variety of values reported for the bio-based films developed for food packaging applications. While some researchers have developed hydrophilic food packaging films with a contact angle below 90 °C (Lee et al., 2024), others have reported developing hydrophobic food packaging films with a contact angle above 90 °C (Zhu et al., 2024). The choice between hydrophobic and hydrophilic surfaces for food packaging depends on the specific requirements and characteristics of the food product being packaged. For instance, hydrophobic surfaces repel water, making them ideal for packaging foods that need to remain dry and crispy, such as snacks, cereals, and crackers. Additionally, materials with low wettability can help inhibit microbial attachment and growth, thus contributing to food safety. On the other hand, hydrophilic surfaces absorb water, which can be beneficial for packaging that needs to manage internal moisture levels, such as certain fresh produce that releases water vapor. Furthermore, hydrophilic materials can absorb moisture from the environment, aiding in quicker degradation, which is useful for environmentally friendly packaging solutions.

### 3.7. Degradation study

The degradability of food packaging films is important in the current era of environmental awareness and sustainability. Thus, the degradation percentage of the fabricated films was assessed over a four-week period using a soil burial degradation test, with the results summarized in Table 2. Additionally, SEM images from the surface of degraded films were provided to visually evaluate the extent of degradation and any changes in film morphology after four weeks, as depicted in Fig. 5A.

**Table 2**  
Soil burial degradation test results for four weeks.

Sample	Week 1 (%)	Week 2 (%)	Week 3 (%)	Week 4 (%)
CMC	33.6 ± 1.4	40.8 ± 2.1	46.7 ± 1.8	50.5 ± 3.1
CMC-C1	25.3 ± 1.0	29.0 ± 1.5	35.8 ± 1.4	47.6 ± 2.9
CMC-C3	17.3 ± 0.7	28.6 ± 1.5	32.7 ± 1.3	40.9 ± 2.5
CMC-C5	17.2 ± 0.7	26.7 ± 1.4	32.3 ± 1.3	39.7 ± 2.5
CMC-C3-P25	14.5 ± 0.6	18.8 ± 0.9	27.6 ± 1.0	34.9 ± 2.1
CMC-C3-P50	11.9 ± 0.5	18.0 ± 0.9	27.1 ± 1.0	31.1 ± 1.9

For comparison, the SEM image of the surface of the films before the degradation test is included in Fig. 5B.

In all cases, the highest degradation rate was observed after the first week, followed by a gradual decrease over time. Initially, the films were fully exposed to the soil environment, facilitating rapid colonization by soil microorganisms such as bacteria, fungi, and actinomycetes. These microorganisms utilize the film as a carbon source, thereby accelerating the degradation process. Moreover, at the onset of the test, the film surface was readily accessible to soil microorganisms, facilitating enzymatic degradation of the cellulose polymer chains. As the test progressed and degradation occurred, the available surface area for microbial colonization diminished, resulting in a reduction in the degradation rate. Specifically, after one week, the observed degradation rate for the CMC film was 33.6 ± 1.4%. The incorporation of clay particles into the CMC matrix led to a reduction in the degradation rate, dropping to 17.3 ± 0.7% in CMC-C3 composite films. Furthermore, with the addition of PE, degradation was further minimized; for instance, CMC-C3-P50 exhibited only 11.9 ± 0.5% degradation after one week. The introduction of clay particles may create a physical barrier, as observed in previous WVP and ORT results, limiting the access of soil microorganisms to the cellulose substrate. Additionally, clay particles often possess hydrophobic surfaces, as evidenced in contact angle results, which can repel water and hinder microbial colonization and activity. Consequently, the presence of clay particles in the CMC film may reduce moisture absorption and create an environment less conducive to microbial degradation, thereby decreasing the degradation rate.

On the other hand, PE contains bioactive compounds such as polyphenols, flavonoids, and tannins, which exhibit antimicrobial properties, as discussed later. These compounds can inhibit the growth and activity of soil microorganisms responsible for cellulose degradation, thus reducing the overall degradation rate of the composite films. Additionally, PE is known for its antioxidant properties, which can mitigate oxidative degradation processes. By scavenging free radicals and reactive oxygen species generated during degradation, PE may protect the CMC matrix from oxidative damage and degradation, leading to enhanced stability and reduced degradation rates.

The SEM images captured from the surface of the films prior to the degradation test, as illustrated in Fig. 5B, exhibited a smooth and homogeneous texture characteristic. However, the degraded samples after four weeks, as shown in Fig. 5A, revealed signs of surface erosion characterized by irregularities, pits, or cavities, suggesting physical breakdown and material loss due to microbial activity or environmental factors (W. Wang, Li, et al., 2024). Moreover, cellulose fibers in the film appeared fragmented or partially degraded, with visible breaks and discontinuities along their length, indicating enzymatic degradation of cellulose polymer chains by microbial enzymes, resulting in fiber structure breakdown.

### 3.8. Antioxidant activity and antibacterial property

Oxygen, an essential element crucial for the metabolism of aerobic organisms, plays a dual role in biological systems. While vital for cellular processes, its reactivity can result in the formation of free radicals, known as reactive oxygen species (ROS). These ROS have the potential to interact with various biomolecules, including proteins, lipids, DNA, and RNA, causing damage that compromises their structure and function. However, the integration of antioxidants into food packaging materials serves as a defense mechanism against oxidative stress induced by ROS. Antioxidants play a critical role in preventing or slowing down the oxidation process, thus preserving the quality and prolonging the shelf life of packaged food products (Soleimanzadeh et al., 2024).

The antioxidant activity (AOA) of the PE-containing composite films was assessed using the DPPH radical scavenging test, with the CMC-C3 composite film serving as a control sample. The AOA of the films at different time intervals—30 min, 1 h, 2 h, 3 h, and 24 h—is illustrated in Fig. 6a. Additionally, Fig. 6b showcases digital images of DPPH solutions

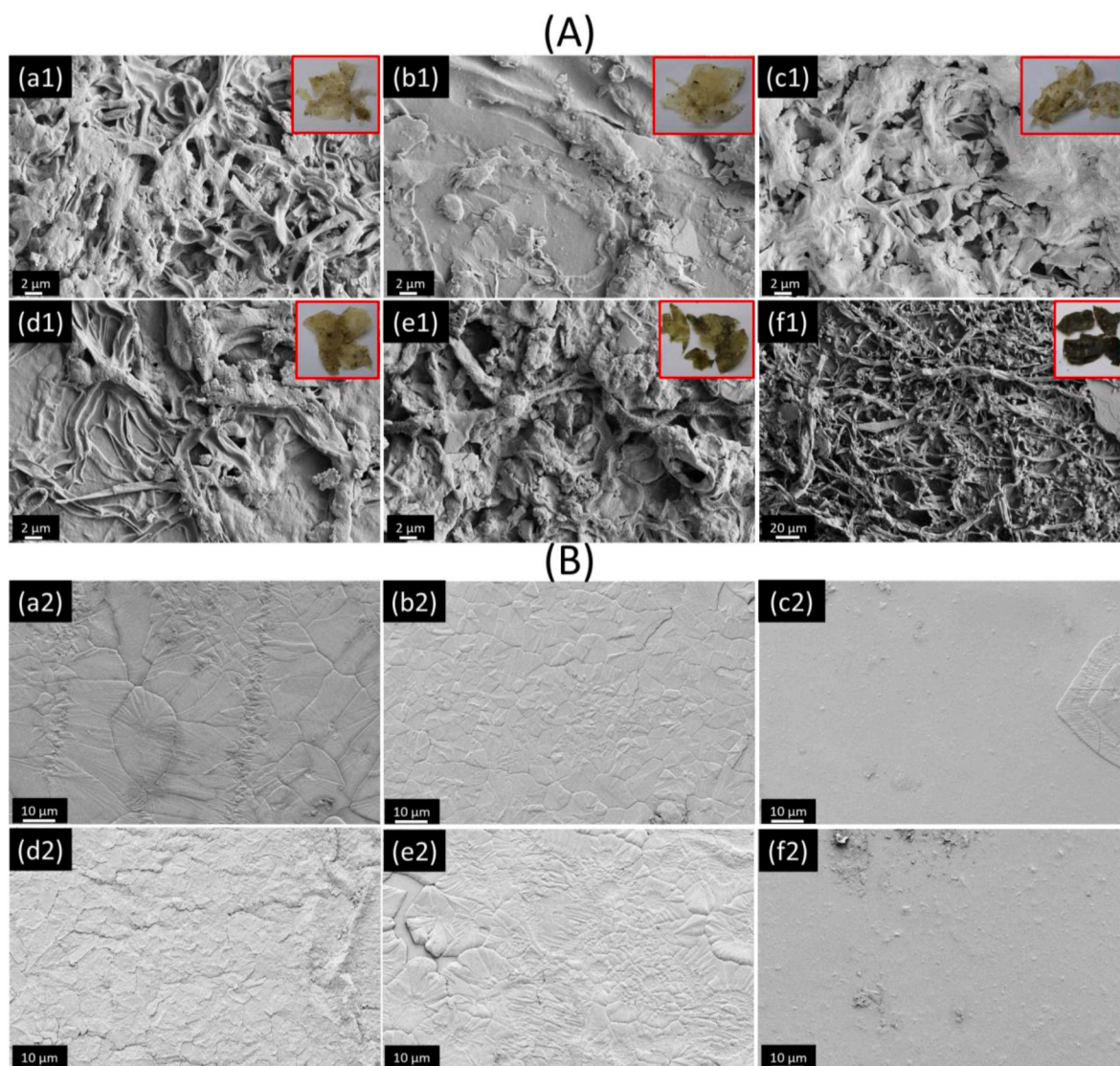


Fig. 5. (A) Digital photos and SEM images of the surface of the degraded samples after 4 weeks: (a1) CMC, (b1) CMC-C1, (c1) CMC-C3, (d1) CMC-C5, (e1) CMC-C3-P25, and (f1) CMC-C3-P50. (B) SEM image from the surface of films before degradation test: (a2) CMC, (b2) CMC-C1, (c2) CMC-C3, (d2) CMC-C5, (e2) CMC-C3-P25, and (f2) CMC-C3-P50.

after 24 h of incubation with the fabricated films, while Fig. 6c presents the UV-vis spectra of pure DPPH solution and DPPH solution after 24 h of incubation with the CMC-C3-P50 composite film. The control sample demonstrated an AOA of  $8.15 \pm 0.4\%$  after 24 h. Although cellulose itself is not conventionally considered an antioxidant, the presence of glycerol as a plasticizer and citric acid as a crosslinker in the CMC film formulation may contribute to the observed AOA. Glycerol contains hydroxyl groups capable of scavenging free radicals and inhibiting oxidative reactions (Kowalska et al., 2021). Additionally, citric acid has been reported to exhibit antioxidant activity by chelating metal ions and scavenging free radicals (Ryan et al., 2019). Following the incorporation of PE, the AOA significantly increased. Specifically, after 24 h, the AOA increased to  $70.3 \pm 2.5\%$  and  $91.0 \pm 3.3\%$  in CMC-C3-PE25 and CMC-C3-PE50, respectively. This enhancement, consistent with findings from other researchers who utilized PE in developing food packaging (Cava et al., 2024; Ranjbar et al., 2024; Vargas-Torrico et al., 2024), underscores the potent antioxidant properties of PE and its effectiveness in enhancing the antioxidant activity of CMC-based films.

Studies have demonstrated that PE exhibits robust antioxidant activity due to its rich content of bioactive compounds such as phenolic compounds, flavonoids, anthocyanins, and tannins. These constituents

possess significant scavenging abilities against free radicals and ROS, effectively neutralizing their harmful effects on cellular structures. Furthermore, PE demonstrates metal-chelating properties, thus inhibiting metal-catalyzed oxidation reactions. Its anti-inflammatory effects further mitigate oxidative stress by inhibiting inflammatory mediators and enzymes. Moreover, the extract enhances endogenous antioxidant defenses by upregulating the activity of key antioxidant enzymes. These combined actions not only protect cells and tissues from oxidative damage but also confer health benefits such as cardiovascular protection, diabetes management, cancer prevention, and neuroprotection (Makhathini et al., 2023; Nabeel Ahmad et al., 2024; Siddiqui et al., 2024; Soleimanzadeh et al., 2024).

In conclusion, the AOA results confirm that the synergistic effects of PE with CMC-based materials represent a promising approach for developing functional food packaging solutions capable of combating oxidative stress and enhancing the stability of packaged products throughout their shelf life.

The results of the antimicrobial activity of CMC-based films against *E. coli*, *S. aureus*, and *L. monocytogenes* are presented in Table 3. No inhibition zone was observed for the CMC and CMC-C3 control films against the tested bacteria. Additionally, no inhibition zone was

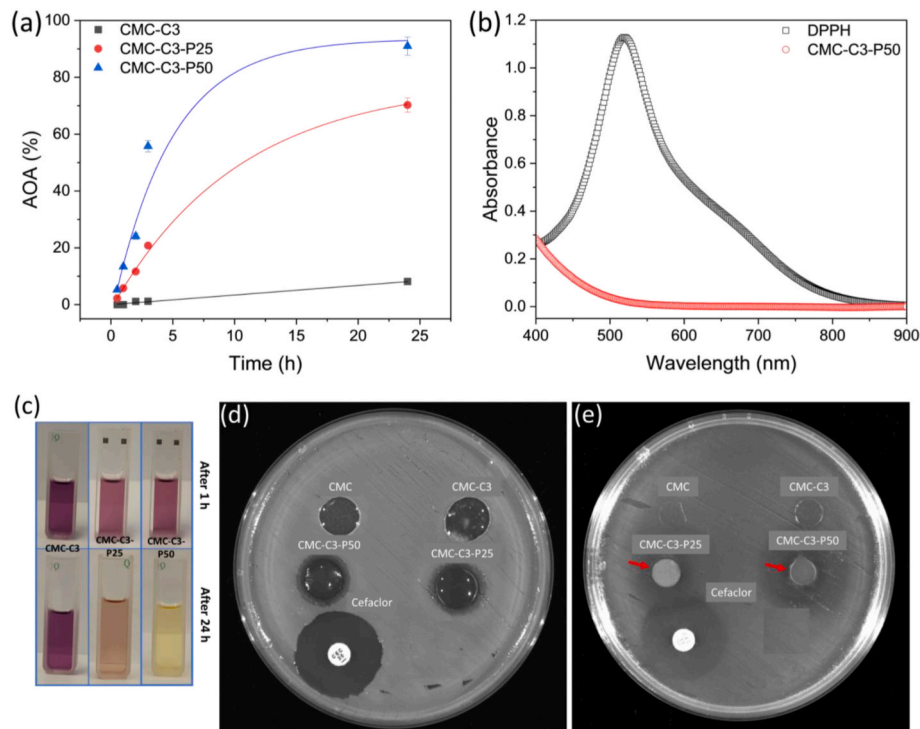


**Fig. 6.** (a) Antioxidant activity (AOA) of the various samples versus time. (b) UV-vis spectra of pure DPPH solution and DDPH solution after 24 h of incubation with the CMC-C3-P50 film. (c) Photograph of the DPPH solutions after 24 h of incubation with the fabricated films. (d) *S. aureus* and (e) *L. monocytogenes*. Red arrows highlight zones of inhibition formed. Photos were taken using ChemiDoc MP imaging system (Biorad) and are representative of one assay.

**Table 3**

Antibacterial activity of CMC, CMC-C3, and PE-containing films determined by agar diffusion assay.

Samples	Zone of inhibition (in mm) <sup>a</sup>		
	<i>E. coli</i> ATCC 25922	<i>S. aureus</i> ATCC 29213	<i>L. monocytogenes</i> DSM 112142
CMC	–	–	–
CMC-C3	–	–	–
CMC-C3-P25	–	3.48 ± 0.97 a	3.66 ± 1.78 a
CMC-C3-P50	–	5.90 ± 1.01 b	3.74 ± 1.57 a
Cefaclor (30 µg)	16.00 ± 1.19	18.53 ± 0.76 c	16.90 ± 1.74 b

<sup>a</sup> Averages (± standard deviation) were calculated from three experiments conducted in triplicate. Zones of inhibition (in mm) exclude the diameter of the disc. Different letters within the same bacterial group indicate significant differences between averages ( $p < 0.05$ ). –: no zone of growth inhibition observed.

observed for the CMC-C3-P25 and CMC-C3-P50 films against *E. coli* (Fig. S4). This observation may be attributed to the gram-negative nature of this bacterial species, which possesses an additional external lipopolysaccharide membrane, rendering it generally more resistant to antimicrobial therapy. However, PE-containing films CMC-C3-P25 and CMC-C3-P50 exhibited antimicrobial activity against *S. aureus* and *L. monocytogenes*, with inhibition zones ranging from 3.48 to 5.90 mm and 3.66–3.74 mm, respectively (Table 3, Fig. 6d and e). Notably, for *S. aureus*, a significant increase in effectiveness (i.e., 1.7-fold) was observed when the PE concentration was doubled ( $p < 0.05$ ). These results strongly indicate the antimicrobial efficacy of PE, consistent with findings reported by other authors (Nozohour et al., 2018; Polat Yemis et al., 2019; Valdés et al., 2019). The presence of polyphenolic compounds in PE, including phenols, tannins, and flavonoids, has been linked to its antimicrobial activity (Kharchoufi et al., 2018; Pagliarulo et al., 2016; Yuan et al., 2015). Studies have also shown that films incorporating pomegranate peels exhibit greater effectiveness against

gram-positive (*S. aureus* and *L. monocytogenes*) compared to gram-negative bacteria (*E. coli*, *Salmonella enterica*) (Ali et al., 2019; Hanani et al., 2019). Furthermore, previous researchers have demonstrated higher antimicrobial activity of pomegranate against *S. aureus* (Dahham et al., 2010; Valdés et al., 2019), corroborating our findings.

### 3.9. Environmental impact determination

An LCA study was undertaken to ascertain whether the renewable and organic-waste-derived nature of the active packaging films developed herein translates into materials with reduced environmental impact (Hermann et al., 2010; Lizundia et al., 2022; RCI's Scientific Background Report: "Case Studies Based on Peer-Reviewed Life Cycle Assessments – Carbon Footprints of Different Carbon-Based Chemicals and Materials" (November 2023), n.d.). The assessment focused on climate change potential, quantified in terms of CO<sub>2</sub> equivalent emissions, in alignment with the plastic packaging industry's decarbonization and carbon neutrality objectives. Results indicate that when utilizing a fossil-based medium voltage electricity mix (European average), the cradle-to-gate climate change potential amounts to 25.9 and 33.2 kg·CO<sub>2</sub> equiv·kg<sup>-1</sup> for neat CMC and CMC-3-P50 films, respectively. As depicted in Fig. 7a, the fabrication of nanocomposite films entails a progressive increase in greenhouse gas emissions stemming from the utilization of additional materials and heightened energy consumption for nanocomposite production. Notably, electricity emerges as the primary contributor to the climate change potential across all formulations, accounting for 82.0%–86.5% of the total (Fig. 7b-left). This is followed by CMC acquisition (7.8%–10.2%) and PE (7.0%–13.2% for CMC-3-P25 and CMC-3-P50 films, respectively).

When utilizing a medium voltage electricity mix sourced from fully renewable sources, the environmental impacts are notably diminished to 4.4–4.8 kg·CO<sub>2</sub> equiv·kg<sup>-1</sup> for pure CMC and CMC-3-P50 films, respectively. This substantial reduction can be attributed to the lower environmental impacts associated with renewable energy sources (see Table S5). As illustrated in Fig. 7b-right, in this scenario, electricity

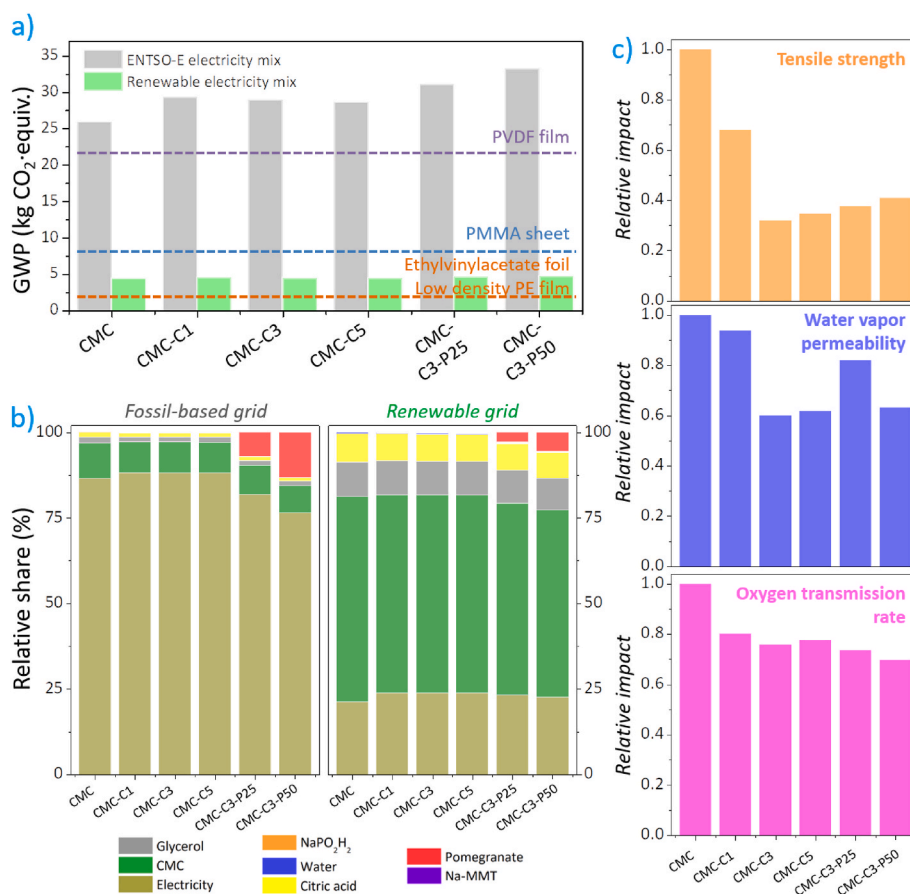


Fig. 7. Environmental impact of bio-based active packaging films: (a) Global Warming Potential, quantified in kg CO<sub>2</sub> equivalents per kilo film, using ENTSO-E and a fully renewable electricity mix; (b) relative contribution to GWP using ENTSO-E and a fully renewable electricity mix. (c) Normalized GWP for a renewable energy mix scenario according to the functional properties of the films, TS, WVP, and OTR.

constitutes 21.3%–23.8% of the total greenhouse gas emissions, with increased contributions from CMC, glycerol, citric acid, and pomegranate. Consequently, the materials developed here possess the necessary attributes to be manufactured with a carbon footprint below 5 kg CO<sub>2</sub> eq./kg, a likely scenario given future global renewable energy targets (*Triple Renewables Target within Reach after Energy Surge – plus Other Top Energy Stories*, n.d.). For comparison with petroleum-derived plastic films, Fig. 7a illustrates comparable or significantly lower climate change potentials: 4.1 kg-CO<sub>2</sub> equiv.·kg<sup>-1</sup> for ethyl vinyl acetate foil and low-density polyethylene packaging film, 9.1 kg-CO<sub>2</sub> equiv.·kg<sup>-1</sup> for polymethyl methacrylate sheet, and 21.2 kg-CO<sub>2</sub> equiv.·kg<sup>-1</sup> for polyvinyl fluoride film (further details in Table S7). Furthermore, as shown in Table S8, relatively similar carbon footprint values are observed when compared to the technologically mature production of bio-based blends with potential packaging applications. These include starch/polylactic, starch/polyvinyl alcohol, and starch/polyethylene blends with 100%, 45%, and 34% biogenic carbon, respectively (2.4–3.1 kg CO<sub>2</sub> eq./kg). Consequently, the LCA results underscore the potential of CMC-based films for sustainable packaging applications.

For a more equitable comparison among the nanocomposites, the environmental impacts associated with a renewable energy mix were standardized based on the functional properties of the films. To accomplish this, the tensile strength (TS), WVP, and OTR were taken into account. As depicted in Fig. 7c, the normalized impacts, relative to the base material and neat CMC film, undergo substantial reductions upon the inclusion of clay and PE. Notably, the most significant reductions in impact are observed when considering mechanical properties, with reductions of up to 59% for the CMC-C3 formulation attributable to the mechanical reinforcing effect of the nanofillers.

Moreover, impacts normalized to WVP exhibit reductions of 40%, while OTR-based climate change impact is reduced by a maximum of 30% (in the case of the CMC-C3-P50 film). Overall, the LCA findings underscore that the incorporation of clay and PE yields materials with enhanced functional properties while also delivering additional environmental benefits pertinent to end-use applications.

For a more comprehensive understanding, additional environmental impact metrics were analyzed, and the findings are summarized in Table 4. Overall, the production of nanocomposite films results in 7%–30% higher impacts (varying by category) for a functional unit of 1 kg compared to pure CMC. This trend is evident across significant impact categories such as acidification, ecotoxicity, land use, particulate matter formation, and water use. Notably, water use increases from 1.11 to 1.45 m<sup>3</sup> when the CMC film is reinforced with clay and PE (CMC-C3-P50 formulation). Additionally, the cumulative energy demand (CED), a critical resource-oriented indicator encompassing the energy consumed during the extraction, manufacturing, and disposal of raw and auxiliary materials, demonstrates similar outcomes across all formulations (1 kg film) when considering the non-renewable component. Notably, the non-renewable CED for the developed films remains approximately 55–58 MJ equiv.·kg<sup>-1</sup>, markedly lower than the 99–244 MJ equiv.·kg<sup>-1</sup> observed for benchmark petroleum-derived films (refer to Table S7). However, an increase in the renewable CED is observed for the nanocomposite films, attributed to the additional energy required and the utilization of PE. Moreover, for certain categories, greater impacts are observed compared to bio-based blends (Table S8), highlighting the need for a holistic understanding of all environmental impact categories when designing sustainable materials for food packaging.

**Table 4**

Environmental impact indicators were obtained using ReCiPe 2016 Midpoint (H) and Cumulative Energy Demand (CED) methodologies for bio-based active packaging films. A 100% renewable energy mix scenario is used.

	Impact category	CMC	CMC-C1	CMC-C3	CMC-C5	CMC-C3-P25	CMC-C3-P50	Unit
ReCiPe 2016 Midpoint (H)	Acidification: terrestrial	0.0190	0.0196	0.0194	0.0192	0.0199	0.0203	kg SO <sub>2</sub> -Eq
	Climate change	4.4429	4.5669	4.5179	4.4699	4.6382	4.7581	kg CO <sub>2</sub> -Eq
	Ecotoxicity: freshwater	0.6258	0.6978	0.6897	0.6817	0.7356	0.7813	kg 1,4-DCB-Eq
	Ecotoxicity: marine	0.8332	0.9266	0.9158	0.9053	0.9761	1.0361	kg 1,4-DCB-Eq
	Ecotoxicity: terrestrial	68.5442	74.9735	74.1342	73.3144	78.8641	83.5755	kg 1,4-DCB-Eq
	Energy resources: non-renewable, fossil	1.0917	1.1074	1.0953	1.0835	1.1155	1.1355	kg oil-Eq
	Eutrophication: freshwater	0.0015	0.0016	0.0015	0.0015	0.0016	0.0016	kg P-Eq
	Eutrophication: marine	0.0013	0.0013	0.0013	0.0012	0.0013	0.0013	kg N-Eq
	Human toxicity: carcinogenic	1.4284	1.5602	1.5424	1.5251	1.6318	1.7208	kg 1,4-DCB-Eq
	Human toxicity: non-carcinogenic	7.7283	8.2624	8.1687	8.0771	8.5322	8.8943	kg 1,4-DCB-Eq
	Ionising radiation	0.2571	0.2603	0.2573	0.2543	0.2604	0.2635	kBq Co-60-Eq
	Land use	1.9354	2.0473	2.0234	2.0001	2.0978	2.1718	m <sup>2</sup> ·a crop-Eq
	Material resources: metals/minerals	0.3172	0.3246	0.3209	0.3173	0.3267	0.3324	kg Cu-Eq
	Ozone depletion	0.0000	0.0000	0.0000	0.0000	0.0000	0.0000	kg CFC-11-Eq
	Particulate matter formation	0.0078	0.0081	0.0080	0.0079	0.0082	0.0083	kg PM2.5-Eq
	Photochemical oxidant formation: human health	0.0109	0.0113	0.0112	0.0110	0.0115	0.0118	kg NO <sub>x</sub> -Eq
	Photochemical oxidant formation: terrestrial ecosyst.	0.0114	0.0118	0.0117	0.0115	0.0120	0.0123	kg NO <sub>x</sub> -Eq
	Water use	1.1123	1.2682	1.2533	1.2387	1.3504	1.4470	m <sup>3</sup>
	Cumulative Energy Demand	Energy resources: non-renewable	55.5724	56.3520	55.7323	55.1270	56.7191	57.7021
Energy resources: non-renewable, biomass		0.0830	0.0827	0.0817	0.0808	0.0817	0.0816	MJ-Eq
Energy resources: non-renewable, fossil		50.6772	51.3977	50.8352	50.2859	51.7633	52.6878	MJ-Eq
Energy resources: non-renewable, nuclear		4.8121	4.8716	4.8153	4.7603	4.8741	4.9327	MJ-Eq
Energy resources: renewable		303.6104	345.7461	341.6761	337.7009	367.8748	393.9710	MJ-Eq
Energy resources: renewable, biomass		24.2269	24.6936	24.4073	24.1276	24.7340	25.0595	MJ-Eq
Energy resources: renewable, geothermal		0.2037	0.2053	0.2030	0.2007	0.2048	0.2065	MJ-Eq
Energy resources: renewable, geothermal, solar, wind		8.4272	9.5321	9.4201	9.3106	10.1107	10.7987	MJ-Eq
Energy resources: renewable, solar		0.0102	0.0105	0.0104	0.0103	0.0107	0.0111	MJ-Eq
Energy resources: renewable, water		270.9563	311.5203	307.8487	304.2627	333.0300	358.1128	MJ-Eq
Energy resources: renewable, wind		8.2133	9.3163	9.2067	9.0997	9.8952	10.5811	MJ-Eq
Total		359.1827	402.0981	397.4083	392.8278	424.5939	451.6731	MJ-Eq

#### 4. Conclusions

Developing sustainable, bio-based food packaging is essential for reducing environmental impact and ensuring long-term food system resilience. Our study investigated CMC-based composite films with clay particles and PE for sustainable active food packaging applications. The inclusion of 3 wt% clay significantly enhanced tensile strength by approximately 300% and reduced WVP and OTR by 60% and 30%, respectively, indicating the films' suitability for extending the shelf life of perishable food products. The incorporation of PE notably improved antioxidant activity, increasing from 8.15% to 91% after 24 h, highlighting the films' potential to preserve product quality and freshness actively. The films also exhibited pronounced antibacterial properties against gram-positive bacteria, particularly *S. aureus*, in high PE content films (CMC-C3-PE50). Our LCA showed that the bio-based films had lower environmental impacts compared to petroleum-derived films, with global warming potential values between 4.4 and 4.8 kg CO<sub>2</sub>-equiv. per kg of processed film under a 100% renewable energy mix scenario. When considering the functional properties, the optimized formulation (CMC-C3-P50) achieved reductions of 59%, 37%, and 30% in global warming potential based on tensile strength, water vapor permeability, and oxygen transmission rate, respectively. In conclusion, CMC-based composite films with PE offer a promising solution for sustainable active food packaging, providing enhanced functionality and reduced environmental impact, thus contributing to the advancement of

sustainable packaging practices in the food industry.

#### CRedit authorship contribution statement

**Hossein Baniasadi:** Writing – review & editing, Writing – original draft, Visualization, Supervision, Project administration, Methodology, Investigation, Conceptualization. **Ziba Fathi:** Visualization, Formal analysis. **Erlantz Lizundia:** Writing – review & editing, Writing – original draft, Visualization, Methodology, Funding acquisition, Formal analysis. **Cristina D. Cruz:** Writing – review & editing, Writing – original draft, Visualization, Methodology, Formal analysis. **Roozbeh Abidnejad:** Visualization, Formal analysis. **Mahyar Fazeli:** Writing – original draft. **Päivi Tammela:** Writing – review & editing, Supervision, Funding acquisition. **Eero Kontturi:** Writing – review & editing, Funding acquisition. **Juha Lipponen:** Funding acquisition. **Jukka Niskanen:** Funding acquisition.

#### Declaration of competing interest

The authors declare that they have no known competing financial interests or personal relationships that could have appeared to influence the work reported in this paper.

## Data availability

Data will be made available on request.

## Acknowledgment

The authors would like to acknowledge the funding of the Research Council of Finland, No. 327248 (ValueBiomat). The authors acknowledge financial support from the University of the Basque Country (Convocatoria de ayudas a grupos de investigación GIU21/010). The DDCB unit at the Faculty of Pharmacy, supported by HiLIFE and Bio-center Finland, is gratefully acknowledged for providing access to microbiology facilities and instruments. R.A. and E.K. acknowledge funding from Business Finland Strategic Centres for Science, Technology, and Innovation IMD1/Kontturi. This work made use of Aalto University Bioeconomy Facilities and OtaNano, Nanomicroscopy Center (Aalto-NMC).

## Appendix A. Supplementary data

Supplementary data to this article can be found online at <https://doi.org/10.1016/j.foodhyd.2024.110525>.

## References

- Abdin, M., Naeem, M. A., & Aly-Aldin, M. M. (2024). Enhancing the bioavailability and antioxidant activity of natamycin E235–ferulic acid loaded polyethylene glycol/carboxy methyl cellulose films as anti-microbial packaging for food application. *International Journal of Biological Macromolecules*, 266, Article 131249. <https://doi.org/10.1016/j.ijbiomac.2024.131249>
- Afshar, S., & Baniasadi, H. (2018). Investigation the effect of graphene oxide and gelatin/starch weight ratio on the properties of starch/gelatin/GO nanocomposite films: The RSM study. *International Journal of Biological Macromolecules*, 109. <https://doi.org/10.1016/j.ijbiomac.2017.11.083>
- Äkräs, L., Silvenius, F., Baniasadi, H., Vahvaselkä, M., Ilvesniemi, H., & Seppälä, J. (2024). A cradle-to-gate life cycle assessment of polyamide-starch biocomposites: Carbon footprint as an indicator of sustainability. *Clean Technologies and Environmental Policy*, 1–16.
- Ali, A., Chen, Y., Liu, H., Yu, L., Baloch, Z., Khalid, S., Zhu, J., & Chen, L. (2019). Starch-based antimicrobial films functionalized by pomegranate peel. *International Journal of Biological Macromolecules*, 129, 1120–1126.
- Alkassafary, A. N., Yassin, M. A., Abdel Rehim, M. H., Liu, L., Jiao, Z., Wang, B., & Wei, Z. (2024). Modified cellulose nanocrystals enhanced polycaprolactone multifunctional films with barrier, UV-blocking and antimicrobial properties for food packaging. *International Journal of Biological Macromolecules*, 261, Article 129871. <https://doi.org/10.1016/j.ijbiomac.2024.129871>
- Asgher, M., Qamar, S. A., Bilal, M., & Iqbal, H. M. N. (2020). Bio-based active food packaging materials: Sustainable alternative to conventional petrochemical-based packaging materials. *Food Research International*, 137, Article 109625. <https://doi.org/10.1016/j.foodres.2020.109625>
- Atta, O. M., Manan, S., Shahzad, A., Ul-Islam, M., Ullah, M. W., & Yang, G. (2022). Biobased materials for active food packaging: A review. *Food Hydrocolloids*, 125, Article 107419. <https://doi.org/10.1016/j.foodhyd.2021.107419>
- Bahmanyar, M., Ramazani, S. A. A., & Baniasadi, H. (2015). Preparation and properties of ethylene-vinyl acetate/linear low-density polyethylene/graphene oxide nanocomposite films. *Polymer - Plastics Technology and Engineering*, 54(11). <https://doi.org/10.1080/03602559.2014.1003231>
- Baniasadi, H., Trifol, J., Lipponen, S., & Seppälä, J. (2021). Sustainable composites of surface-modified cellulose with low-melting point polyamide. *Materials Today Chemistry*, 22, Article 100590.
- Basbasan, A. J., Hararak, B., Winotapun, C., Wanmolee, W., Leelaphiwat, P., Boonruang, K., Chinsirikul, W., & Chonhenchob, V. (2022). Emerging challenges on viability and commercialization of lignin in biobased polymers for food packaging: A review. *Food Packaging and Shelf Life*, 34, Article 100969. <https://doi.org/10.1016/j.foodres.2022.100969>
- Behnezhad, M., Goodarzi, M., & Baniasadi, H. (2020). Fabrication and characterization of polyvinyl alcohol/carboxymethyl cellulose/titanium dioxide degradable composite films: An RSM study. *Materials Research Express*, 6(12), Article 125548.
- Berrocchi, M., Vallejo, C., & Lizundia, E. (2022). Environmental impact assessment of chitin nanofibril and nanocrystal isolation from fungi, shrimp shells, and crab shells. *ACS Sustainable Chemistry & Engineering*, 10(43), 14280–14293.
- Bertolo, M. R. V., Dias, L. D., Oliveira Filho, J. G. de, Alves, F., Marangon, C. A., Amaro Martins, V. da C., Ferreira, M. D., Bagnato, V. S., Guzzi Plepis, A. M. de, & Bogusz, S. (2022). Central composite design optimization of active and physical properties of food packaging films based on chitosan/gelatin/pomegranate peel extract. *Food Packaging and Shelf Life*, 34, Article 100986. <https://doi.org/10.1016/j.foodres.2022.100986>
- Bodana, V., Swer, T. L., Kumar, N., Singh, A., Samtiya, M., Sari, T. P., & Babar, O. A. (2024). Development and characterization of pomegranate peel extract-functionalized jackfruit seed starch-based edible films and coatings for prolonging the shelf life of white grapes. *International Journal of Biological Macromolecules*, 254, Article 127234. <https://doi.org/10.1016/j.ijbiomac.2023.127234>
- Bovea, M. D., & Pérez-Belis, V. (2012). A taxonomy of ecodesign tools for integrating environmental requirements into the product design process. *Journal of Cleaner Production*, 20(1), 61–71.
- Cava, R., Ladero, L., Riaguas, E., & Vidal-Aragón, M. C. (2024). Assessing the impact of pomegranate peel extract active packaging and high Hydrostatic pressure processing on color and oxidative stability in sliced Nitrate/Nitrite-reduced Iberian dry-cured loins. *Foods*, 13(3), 360.
- Chakraborty, P., Hati, S., & Mishra, B. K. (2023). Biocomposite films from banana flour/halloysite nanoclay/carvacrol: Preparation, characterization, and application on capsicum (Capsicum annum) fruits. *Sustainable Chemistry and Pharmacy*, 36, Article 101304. <https://doi.org/10.1016/j.scp.2023.101304>
- CLSI M02-A12 and CLSI M100-S26. (n.d.). <https://webstore.ansi.org/standards/cls/clsim02a12m100s26>.
- Cui, H., Surendhiran, D., Li, C., & Lin, L. (2020). Biodegradable zein active film containing chitosan nanoparticle encapsulated with pomegranate peel extract for food packaging. *Food Packaging and Shelf Life*, 24, Article 100511. <https://doi.org/10.1016/j.foodres.2020.100511>
- Dahham, S. S., Ali, M. N., Tabassum, H., & Khan, M. (2010). Studies on antibacterial and antifungal activity of pomegranate (*Punica granatum* L.). *American-Eurasian Journal of Agricultural & Environmental Sciences*, 9(3), 273–281.
- de Cuadro, P., Belt, T., Kontturi, K. S., Reza, M., Kontturi, E., Vuorinen, T., & Hughes, M. (2015). Cross-linking of cellulose and poly(ethylene glycol) with citric acid. *Reactive and Functional Polymers*, 90, 21–24. <https://doi.org/10.1016/j.reactfunctpolym.2015.03.007>
- Dharini, V., Periyar Selvam, S., Jayaramudu, J., & Sadiku Emmanuel, R. (2022). Functional properties of clay nanofillers used in the biopolymer-based composite films for active food packaging applications - review. *Applied Clay Science*, 226, Article 106555. <https://doi.org/10.1016/j.clay.2022.106555>
- Dinesh, Wang, H., & Kim, J. (2022). Citric acid-crosslinked highly porous cellulose nanofiber foam prepared by an environment-friendly and simple process. *Global Challenges*, 6(11), Article 2200090.
- El Bourakadi, K., Qaiss, A. el kacem, & Bouhfid, R. (2022). Bio-films based on alginate/modified clay through spray drying: Mechanical, rheological, morphological, and transport properties for potential use as active food packaging. *International Journal of Biological Macromolecules*, 210, 663–668. <https://doi.org/10.1016/j.ijbiomac.2022.04.222>
- El Mouzahim, M., Eddarai, E. M., Eladaoui, S., Guenbour, A., Bellaouchou, A., Zarrouk, A., & Boussen, R. (2023). Food packaging composite film based on chitosan, natural kaolinite clay, and *Ficus. carica* leaves extract for fresh-cut apple slices preservation. *International Journal of Biological Macromolecules*, 233, Article 123430. <https://doi.org/10.1016/j.ijbiomac.2023.123430>
- El-Shall, F. N., Al-Shemy, M. T., & Dawwam, G. E. (2023). Multifunction smart nanocomposite film for food packaging based on carboxymethyl cellulose/Kombucha SCOBY/pomegranate anthocyanin pigment. *International Journal of Biological Macromolecules*, 242, Article 125101. <https://doi.org/10.1016/j.ijbiomac.2023.125101>
- Elmahdy, M. M., & Yassin, M. A. (2024). Linear and nonlinear optical parameters of biodegradable chitosan/polyvinyl alcohol/sodium montmorillonite nanocomposite films for potential optoelectronic applications. *International Journal of Biological Macromolecules*, 258, Article 128914. <https://doi.org/10.1016/j.ijbiomac.2023.128914>
- Fazeli, M. (2018). *Development of hydrophobic thermoplastic starch composites*.
- Fernández-Santos, J., Valls, C., Cusola, O., & Roncero, M. B. (2022). Composites of cellulose nanocrystals in combination with either cellulose nanofibril or carboxymethylcellulose as functional packaging films. *International Journal of Biological Macromolecules*, 211, 218–229. <https://doi.org/10.1016/j.ijbiomac.2022.05.049>
- Gironi, F., & Piemonte, V. (2011). Life cycle assessment of polylactic acid and polyethylene terephthalate bottles for drinking water. *Environmental Progress & Sustainable Energy*, 30(3), 459–468.
- Godoy Zúñiga, M. M., Ding, R., Oh, E., Nguyen, T. B., Tran, T. T., Nam, J.-D., & Suhr, J. (2024). Avocado seed starch utilized in eco-friendly, UV-blocking, and high-barrier polylactic acid (PLA) biocomposites for active food packaging applications. *International Journal of Biological Macromolecules*, 265, Article 130837. <https://doi.org/10.1016/j.ijbiomac.2024.130837>
- Gopalakrishnan, K., Chandel, M., Gupta, V., Kaur, K., Patel, A., Kaur, K., Kishore, A., Prabhakar, P. K., Singh, A., Shankar Prasad, J., Bodana, V., Saxena, V., Shanmugam, V., & Sharma, A. (2023). Valorisation of fruit peel bioactive into green synthesized silver nanoparticles to modify cellulose wrapper for shelf-life extension of packaged bread. *Food Research International*, 164, Article 112321. <https://doi.org/10.1016/j.foodres.2022.112321>
- Hanani, Z. A. N., Yee, F. C., & Nor-Khaizura, M. A. R. (2019). Effect of pomegranate (*Punica granatum* L.) peel powder on the antioxidant and antimicrobial properties of fish gelatin films as active packaging. *Food Hydrocolloids*, 89, 253–259.
- Hellweg, S., & Milà i Canals, L. (2014). Emerging approaches, challenges and opportunities in life cycle assessment. *Science*, 344(6188), 1109–1113.
- Hermann, B. G., Blok, K., & Patel, M. K. (2010). Twisting biomaterials around your little finger: Environmental impacts of bio-based wrappings. *International Journal of Life Cycle Assessment*, 15, 346–358.
- Hou, M., Xia, B., Qu, R., Dong, J., Li, T., Wang, S., Wang, Y., & Dong, W. (2024). Preparation of the double cross-linking carbon dots-polyvinyl alcohol-

- carboxymethyl cellulose composite film for food active packaging application. *International Journal of Biological Macromolecules*, 273, Article 132939. <https://doi.org/10.1016/j.ijbiomac.2024.132939>
- Iturrondobaitia, M., Vallejo, C., Berruci, M., Akizu-Gardoki, O., Minguez, R., & Lizundia, E. (2022). Environmental impact assessment of LiNi<sub>1</sub>/3Mn<sub>1</sub>/3Co<sub>1</sub>/3O<sub>2</sub> hydrometallurgical cathode recycling from spent lithium-ion batteries. *ACS Sustainable Chemistry & Engineering*, 10(30), 9798–9810.
- Jali, S., Mohan, T. P., Mwangi, F. M., & Kanny, K. (2023). A review on barrier properties of cellulose/clay nanocomposite polymers for packaging applications. *Polymers*, 16(1), 51.
- Khalid, S. A., Ghanem, A. F., Abd-El-Malek, A., Ammar, M. A., El-khateib, T., & El-Sherbiny, I. M. (2024). Free-standing carboxymethyl cellulose film incorporating nanoformulated pomegranate extract for meat packaging. *Carbohydrate Polymers*, 332, Article 121915. <https://doi.org/10.1016/j.carbpol.2024.121915>
- Khan, S., Hashim, S. B. H., Arslan, M., Zhang, K., Bilal, M., Zhiyang, C., Zhihua, L., Tahir, H. E., Zhai, X., Shishir, M. R. I., & Zou, X. (2024). Berry wax improves the physico-mechanical, thermal, water barrier properties and biodegradable potential of chitosan food packaging film. *International Journal of Biological Macromolecules*, 261, Article 129821. <https://doi.org/10.1016/j.ijbiomac.2024.129821>
- Kharchoufi, S., Parafati, L., Licciardello, F., Muratore, G., Hamdi, M., Cirvilleri, G., & Restuccia, C. (2018). Edible coatings incorporating pomegranate peel extract and biocontrol yeast to reduce *Penicillium digitatum* postharvest decay of oranges. *Food Microbiology*, 74, 107–112.
- Kowalska, G., Baj, T., Kowalski, R., & Szymańska, J. (2021). Optimization of glycerol–water extraction of selected bioactive compounds from peppermint and common nettle. *Antioxidants*, 10(5), 817.
- Kuchaiyaphum, P., Chotichayapong, C., Kajsanthia, K., & Saengsuwan, N. (2024). Carboxymethyl cellulose/poly (vinyl alcohol) based active film incorporated with tamarind seed coat waste extract for food packaging application. *International Journal of Biological Macromolecules*, 255, Article 128203. <https://doi.org/10.1016/j.ijbiomac.2023.128203>
- Kumar, N., Daniloski, D., Pratibha, N., D’Cunha, N. M., Naumovski, N., & Petkoska, A. T. (2022). Pomegranate peel extract – a natural bioactive addition to novel active edible packaging. *Food Research International*, 156, Article 111378. <https://doi.org/10.1016/j.foodres.2022.111378>
- Latif, S., Ahmed, M., Ahmed, M., Ahmad, M., Al-Ahmary, K. M., & Ali, I. (2024). Development of *Plumeria alba* extract supplemented biodegradable films containing chitosan and cellulose derived from bagasse and corn cob waste for antimicrobial food packaging. *International Journal of Biological Macromolecules*, 266, Article 131262. <https://doi.org/10.1016/j.ijbiomac.2024.131262>
- Laurent, A., Weidema, B. P., Bare, J., Liao, X., Maia de Souza, D., Pizzol, M., Sala, S., Schreiber, H., Thonemann, N., & Verones, F. (2020). Methodological review and detailed guidance for the life cycle interpretation phase. *Journal of Industrial Ecology*, 24(5), 986–1003.
- Lee, H.-G., Lee, S. Y., & Yoo, S. (2024). Innovative food-upcycling solutions: Comparative analysis of edible films from kimchi-extracted cellulose, sorbitol, and citric acid for food packaging applications. *Food Chemistry*, 450, Article 139267. <https://doi.org/10.1016/j.foodchem.2024.139267>
- Li, Z., Chen, C., Xie, H., Yao, Y., Zhang, X., Brozena, A., Li, J., Ding, Y., Zhao, X., & Hong, M. (2022). Sustainable high-strength macrofibres extracted from natural bamboo. *Nature Sustainability*, 5(3), 235–244.
- Li, Z., Guan, J., Yan, C., Chen, N., Wang, C., Liu, T., Cheng, F., Guo, Q., Zhang, X., Ye, X., Liu, Y., & Shao, Z. (2023). Corn straw core/cellulose nanofibers composite for food packaging: Improved mechanical, bacteria blocking, ultraviolet and water vapor barrier properties. *Food Hydrocolloids*, 143, Article 108884. <https://doi.org/10.1016/j.foodhyd.2023.108884>
- Li, C., Xia, X., Tan, M., Tao, Y., Lv, Y., Lu, J., Du, J., & Wang, H. (2024). Mechanically robust carboxymethyl cellulose/graphene oxide composite cross-linked by polyetherimide for fruits packaging and preservation system. *International Journal of Biological Macromolecules*, 272, Article 132816. <https://doi.org/10.1016/j.ijbiomac.2024.132816>
- Li, W., Zhang, J., Chen, X., Zhou, X., Zhou, J., Sun, H., Wang, S., & Liu, Y. (2024). Organic nanoparticles incorporated starch/carboxymethylcellulose multifunctional coating film for efficient preservation of perishable products. *International Journal of Biological Macromolecules*, 275, Article 133357. <https://doi.org/10.1016/j.ijbiomac.2024.133357>
- Liu, J., Dong, Y., Zheng, X., Pei, Y., & Tang, K. (2024). Citric acid crosslinked soluble soybean polysaccharide films for active food packaging applications. *Food Chemistry*, 438, Article 138009. <https://doi.org/10.1016/j.foodchem.2023.138009>
- Lizundia, E., Luzi, F., & Puglia, D. (2022). Organic waste valorisation towards circular and sustainable biocomposites. *Green Chemistry*, 24(14), 5429–5459.
- Long, J., Zhang, W., Zhao, M., & Ruan, C.-Q. (2023). The reduce of water vapor permeability of polysaccharide-based films in food packaging: A comprehensive review. *Carbohydrate Polymers*, 321, Article 121267. <https://doi.org/10.1016/j.carbpol.2023.121267>
- Lv, Y., Li, P., Cen, L., Wen, F., Su, R., Cai, J., Chen, J., & Su, W. (2024). Gelatin/carboxymethylcellulose composite film combined with photodynamic antibacterial: New prospect for fruit preservation. *International Journal of Biological Macromolecules*, 257, Article 128643. <https://doi.org/10.1016/j.ijbiomac.2023.128643>
- Majumder, S., Huang, S., Zhou, J., Wang, Y., & George, S. (2023). Tannic acid-loaded halloysite clay grafted with silver nanoparticles enhanced the mechanical and antimicrobial properties of soy protein isolate films for food-packaging applications. *Food Packaging and Shelf Life*, 39, Article 101142. <https://doi.org/10.1016/j.fpsl.2023.101142>
- Makam, R. M. M., Wan Omar, W. N. N., Ahmad, D. A. bin J. @., Nor, N. U. M., Shamjuddin, A., & Amin, N. A. S. (2024). The potential of carboxymethyl cellulose from empty fruit bunch as versatile material in food coating: A review. *Carbohydrate Polymers*, 338, Article 122194. <https://doi.org/10.1016/j.carbpol.2024.122194>
- Makhathini, N., Kaseke, T., & Fawole, O. A. (2023). Microencapsulation of organic pomegranate peel extract for a food circular economy: Effects of wall materials on powder functional attributes, antioxidant activity and antimicrobial property against foodborne pathogens. *Journal of Agriculture and Food Research*, 14, Article 100780. <https://doi.org/10.1016/j.jafr.2023.100780>
- Mao, L., Bai, Z., Yao, J., & Liu, Y. (2022). Development of novel poly(lactic acid) active multilayer composite films by incorporating catechol-functionalized layered clay into chitosan/poly(vinyl alcohol) coatings. *Progress in Organic Coatings*, 170, Article 107000. <https://doi.org/10.1016/j.porgcoat.2022.107000>
- Mohammadpour Velni, S., Baniasadi, H., & Vaziri, A. (2018). Fabrication and characterization of antimicrobial starch-based nanocomposite films and modeling the process parameters via the RSM. *Polymer Composites*, 39. <https://doi.org/10.1002/pc.24733>
- Mukherjee, S., Sengupta, A., Preetam, S., Das, T., Bhattacharya, T., & Thorat, N. (2024). Effects of fatty acid esters on mechanical, thermal, microbial, and moisture barrier properties of carboxymethyl cellulose-based edible films. *Carbohydrate Polymer Technologies and Applications*, 7, Article 100505. <https://doi.org/10.1016/j.carpta.2024.100505>
- Nabel Ahmad, H., Yong, Y., Wang, S., Munawar, N., & Zhu, J. (2024). Development of novel carboxymethyl cellulose/gelatin-based edible films with pomegranate peel extract as antibacterial/antioxidant agents for beef preservation. *Food Chemistry*, 443, Article 138511. <https://doi.org/10.1016/j.foodchem.2024.138511>
- Nath, D., R. S., Pal, K., & Sarkar, P. (2022). Nanoclay-based active food packaging systems: A review. *Food Packaging and Shelf Life*, 31, Article 100803. <https://doi.org/10.1016/j.fpsl.2021.100803>
- Nozohour, Y., Golmohammadi, R., Mirnejad, R., & Fartashvand, M. (2018). Antibacterial activity of pomegranate (*Punica granatum L.*) seed and peel alcoholic extracts on *Staphylococcus aureus* and *Pseudomonas aeruginosa* isolated from health centers. *Journal of Applied Biotechnology Reports*, 5(1), 32–36.
- Pagliarulo, C., De Vito, V., Picariello, G., Colicchio, R., Pastore, G., Salvatore, P., & Volpe, M. G. (2016). Inhibitory effect of pomegranate (*Punica granatum L.*) polyphenol extracts on the bacterial growth and survival of clinical isolates of pathogenic *Staphylococcus aureus* and *Escherichia coli*. *Food Chemistry*, 190, 824–831.
- Peters, J., Buchholz, D., Passerini, S., & Weil, M. (2016). Life cycle assessment of sodium-ion batteries. *Energy & Environmental Science*, 9(5), 1744–1751.
- Polat Yemis, G., Bach, S., & Delaquis, P. (2019). Antibacterial activity of polyphenol-rich pomegranate peel extract against *Cronobacter sakazakii*. *International Journal of Food Properties*, 22(1), 985–993.
- Ramakrishnan, R., Kim, J. T., Roy, S., & Jayakumar, A. (2024). Recent advances in carboxymethyl cellulose-based active and intelligent packaging materials: A comprehensive review. *International Journal of Biological Macromolecules*, 259, Article 129194. <https://doi.org/10.1016/j.ijbiomac.2023.129194>
- Ranjbar, A., Ramezani, A., & Niakousari, M. (2024). Enhancing antioxidant potential and bioactive compounds preservation of ready-to-eat pomegranate arils through modified atmosphere packaging enriched with thymol. *Applied Fruit Science*, 66(2), 739–753.
- RCI’s scientific background report: “Case studies based on peer-reviewed Life Cycle Assessments – Carbon footprints of different carbon-based chemicals and materials” (November 2023). (n.d.). <https://renewable-carbon.eu/publications/product/rci-scientific-background-report-2023/>.
- Riahi, Z., Khan, A., Shin, G. H., Rhim, J.-W., & Kim, J. T. (2024). Sustainable chitosan/polyvinyl alcohol composite film integrated with sulfur-modified montmorillonite for active food packaging applications. *Progress in Organic Coatings*, 192, Article 108474. <https://doi.org/10.1016/j.porgcoat.2024.108474>
- Rochima, E., Octaviani, D., Azhary, S. Y., Prasetyangga, D., Panatarani, C., & Joni, I. M. (2024). Effect of fish gelatin as a structure forming agent to enhance transparency and speed up degradability of bioanocomposite semi-refined kappa carrageenan film reinforced with ZnO and SiO<sub>2</sub> filler. *Food Hydrocolloids*, 152, Article 109965. <https://doi.org/10.1016/j.foodhyd.2024.109965>
- Ryan, E. M., Duryee, M. J., Hollins, A., Dover, S. K., Pirruccello, S., Sayles, H., Real, K. D., Hunter, C. D., Thiele, G. M., & Mikuls, T. R. (2019). Antioxidant properties of citric acid interfere with the uricase-based measurement of circulating uric acid. *Journal of Pharmaceutical and Biomedical Analysis*, 164, 460–466. <https://doi.org/10.1016/j.jpba.2018.11.011>
- Salim, A., Deiana, P., Fancello, F., Molinu, M. G., Santona, M., & Zara, S. (2023). Antimicrobial and antibiofilm activities of pomegranate peel phenolic compounds: Varietal screening through a multivariate approach. *Journal of Bioresources and Bioproducts*, 8(2), 146–161. <https://doi.org/10.1016/j.jobab.2023.01.006>
- Sg, L., Sethi, S., Bk, P., Nayak, S. L., & M, M. (2023). Ornamental plant extracts: Application in food colouration and packaging, antioxidant, antimicrobial and pharmacological potential—A concise review. *Food Chemistry Advances*, 3, Article 100529. <https://doi.org/10.1016/j.focha.2023.100529>
- Shahbazi, M., Ahmadi, S. J., Seif, A., & Rajabzadeh, G. (2016). Carboxymethyl cellulose film modification through surface photo-crosslinking and chemical crosslinking for food packaging applications. *Food Hydrocolloids*, 61, 378–389. <https://doi.org/10.1016/j.foodhyd.2016.04.021>
- Siddiqui, S. A., Singh, S., & Nayik, G. A. (2024). Bioactive compounds from pomegranate peels - biological properties, structure–function relationships, health benefits and food applications – a comprehensive review. *Journal of Functional Foods*, 116, Article 106132. <https://doi.org/10.1016/j.jff.2024.106132>

- Soleimanzadeh, A., Mizani, S., Mirzaei, G., Bavarsad, E. T., Farhoodi, M., Esfandiari, Z., & Rostami, M. (2024). Recent advances in characterizing the physical and functional properties of active packaging films containing pomegranate peel. *Food Chemistry X*, 22, Article 101416. <https://doi.org/10.1016/j.fochx.2024.101416>
- Tanwar, R., Gupta, V., Kumar, P., Kumar, A., Singh, S., & Gaikwad, K. K. (2021). Development and characterization of PVA-starch incorporated with coconut shell extract and sepiolite clay as an antioxidant film for active food packaging applications. *International Journal of Biological Macromolecules*, 185, 451–461. <https://doi.org/10.1016/j.ijbiomac.2021.06.179>
- Triple renewables target within reach after energy surge – Plus other top energy stories. (n.d.). <https://www.weforum.org/agenda/2024/01/energy-transition-renewables-capacity/#:~:text=Under existing policies and market,from current levels by 2030>
- Upadhyay, A., Kumar, P., Kardam, S. K., & Gaikwad, K. K. (2022). Ethylene scavenging film based on corn starch-gum acacia impregnated with sepiolite clay and its effect on quality of fresh broccoli florets. *Food Bioscience*, 46, Article 101556. <https://doi.org/10.1016/j.fbio.2022.101556>
- Valdés, A., García-Serna, E., Martínez-Abad, A., Vilaplana, F., Jiménez, A., & Garrigós, M. C. (2019). Gelatin-based antimicrobial films incorporating pomegranate (*Punica granatum* L.) seed juice by-product. *Molecules*, 25(1), 166.
- Vargas-Torrico, M. F., Aguilar-Méndez, M. A., Ronquillo-de Jesús, E., Jaime-Fonseca, M. R., & von Borries-Medrano, E. (2024). Preparation and characterization of gelatin-carboxymethylcellulose active film incorporated with pomegranate (*Punica granatum* L.) peel extract for the preservation of raspberry fruit. *Food Hydrocolloids*, 150, Article 109677. <https://doi.org/10.1016/j.foodhyd.2023.109677>
- Vargas-Torrico, M. F., von Borries-Medrano, E., & Aguilar-Méndez, M. A. (2022). Development of gelatin/carboxymethylcellulose active films containing Hass avocado peel extract and their application as a packaging for the preservation of berries. *International Journal of Biological Macromolecules*, 206, 1012–1025. <https://doi.org/10.1016/j.ijbiomac.2022.03.101>
- Velásquez, E., de Dicastillo, C. L., Rojas, A., Garrido, L., Pérez, C. J., Lira, M., Guarda, A., & Galotto, M. J. (2024). Multiple mechanical recycling of a post-industrial flexible polypropylene and its nanocomposite with clay: Impact on properties for food packaging applications. *Food Packaging and Shelf Life*, 43, Article 101272. <https://doi.org/10.1016/j.fpsl.2024.101272>
- Viswanathan, V. P., Kulandhaivelu, S. V., Manivasakan, K., & Ramakrishnan, R. (2024). Development of biodegradable packaging films from carboxymethyl cellulose and oxidised natural rubber latex. *International Journal of Biological Macromolecules*, 262, Article 129980. <https://doi.org/10.1016/j.ijbiomac.2024.129980>
- Wang, K., Li, W., Wu, L., Li, Y., & Li, H. (2024). Preparation and characterization of chitosan/dialdehyde carboxymethyl cellulose composite film loaded with cinnamaldehyde@zein nanoparticles for active food packaging. *International Journal of Biological Macromolecules*, 261, Article 129586. <https://doi.org/10.1016/j.ijbiomac.2024.129586>
- Wang, W., Liu, X., Guo, F., Yu, Y., Lu, J., Li, Y., Cheng, Q., Peng, J., & Yu, G. (2024). Biodegradable cellulose/curcumin films with Janus structure for food packaging and freshness monitoring. *Carbohydrate Polymers*, 324, Article 121516. <https://doi.org/10.1016/j.carbpol.2023.121516>
- Yang, J., Li, Y., Liu, B., Wang, K., Li, H., & Peng, L. (2024). Carboxymethyl cellulose-based multifunctional film integrated with polyphenol-rich extract and carbon dots from coffee husk waste for active food packaging applications. *Food Chemistry*, 448, Article 139143. <https://doi.org/10.1016/j.foodchem.2024.139143>
- Yang, Y.-C., Lin, H.-S., Chen, H.-X., Wang, P.-K., Zheng, B.-D., Huang, Y.-Y., Zhang, N., Zhang, X.-Q., Ye, J., & Xiao, M.-T. (2024). Plant polysaccharide-derived edible film packaging for instant food: Rapid dissolution in hot water coupled with exceptional mechanical and barrier characteristics. *International Journal of Biological Macromolecules*, 132066. <https://doi.org/10.1016/j.ijbiomac.2024.132066>
- Yildirim-Yalcin, M., Tornuk, F., & Toker, O. S. (2022). Recent advances in the improvement of carboxymethyl cellulose-based edible films. *Trends in Food Science & Technology*, 129, 179–193. <https://doi.org/10.1016/j.tifs.2022.09.022>
- Yuan, G., Lv, H., Yang, B., Chen, X., & Sun, H. (2015). Physical properties, antioxidant and antimicrobial activity of chitosan films containing carvacrol and pomegranate peel extract. *Molecules*, 20(6), 11034–11045.
- Zeng, J., Ma, Y., Li, P., Zhang, X., Gao, W., Wang, B., Xu, J., & Chen, K. (2024). Development of high-barrier composite films for sustainable reduction of non-biodegradable materials in food packaging application. *Carbohydrate Polymers*, 330, Article 121824. <https://doi.org/10.1016/j.carbpol.2024.121824>
- Zhang, T., Wei, W., Wang, B., Sun, D., Sheng, S., Xu, H., & Wu, M. (2024). A new two-step combined modification method for preparing amylopectin biofilms with high transparency and ideal properties as foods packaging materials. *Food Packaging and Shelf Life*, 42, Article 101248. <https://doi.org/10.1016/j.fpsl.2024.101248>
- Zhu, H., Cheng, J.-H., & Han, Z. (2024). Construction of a sustainable and hydrophobic high-performance all-green pineapple peel cellulose nanocomposite film for food packaging. *International Journal of Biological Macromolecules*, 256, Article 128396. <https://doi.org/10.1016/j.ijbiomac.2023.128396>
- Zia, J., Paul, U. C., Heredia-Guerrero, J. A., Athanassiou, A., & Fragouli, D. (2019). Low-density polyethylene/curcumin melt extruded composites with enhanced water vapor barrier and antioxidant properties for active food packaging. *Polymer*, 175, 137–145. <https://doi.org/10.1016/j.polymer.2019.05.012>